Enantiopure distorted ribbon-shaped nanographene combining two-photon absorption-based upconversion and circularly polarized luminescence

Carlos M. Cruz,[a] Irene R. Márquez,[a] Inês F. A. Mariz,[b] Victor Blanco,[a] Carlos Sánchez-Sánchez,[c] Jesús M. Sobrado,[d] José A. Martín-Gago,[c, d] Juan M. Cuerva,[a] Ermelinda Maçôas*[b] and Araceli G. Campaña*[a]

[a] Departamento de Química Orgánica. Facultad de Ciencias, Universidad de Granada, E-18071 Granada, Spain.
[b] Centro de Química-Física Molecular (CQFM) and Institute of Nanoscience and Nanotechnology (IN), Instituto Superior Técnico, University of Lisbon, Av. Rovisco Pais, 1,1049-001 Lisboa, Portugal.
[c] Instituto de Ciencia de Materiales de Madrid (ICMM-CSIC), Sor Juana Inés de la Cruz 3, 28049 Madrid, Spain.
[d] Centro de Astrobiología INTA-CSIC, Torrejón de Ardoz, 28850 Madrid, Spain.

*E-mail: araceligc@ugr.es, ermelinda.macoas@tecnico.ulisboa.pt

- Electronic Supplementary Information -

Table of Contents

General Details

Unless otherwise stated, all reagents and solvents (CH_2Cl_2, EtOAc, hexane, Et_3N) were purchased from commercial sources and used without further purification. Dry THF was freshly distilled over Na/benzophenone. HPLC grade solvents (hexane, CH_2Cl_2) were purchased from VWR. Dry CH_2Cl_2 was purchased from Sigma-Aldrich. Flash column chromatography was carried out using Silica gel 60 (230-400 mesh, Scharlab, Spain) as the stationary phase. Analytical TLC was performed on aluminium sheets coated with silica gel with fluorescent indicator UV_{254} (Alugram SIL G/UV_{254}, Mackerey-Nagel, Germany) and observed under UV light (254 nm) and/or stained with phosphomolybdic acid (5% methanol solution). All ^{1}H and ^{13}C NMR spectra were recorded on Varian 300, 400 or 500 MHz spectrometers, at a constant temperature of 298 K. Chemical shifts are reported in ppm and referenced to residual solvent. Coupling constants (*J*) are reported in Hertz (Hz). Standard abbreviations indicating multiplicity were used as follows: m = multiplet, quint. = quintet, q = quartet, t = triplet, d = doublet, s = singlet, b = broad. Assignment of the ^{13}C NMR multiplicities was accomplished by DEPT techniques. MALDI-TOF mass spectra were recorded on a Bruker Ultraflex III mass spectrometer. IR-ATR spectra were recorded on a Perkin Elmer Spectrum Two IR Spectrometer. Optical rotations were recorded on a Perkin-Elmer 341 polarimeter at room temperature.

Synthesis

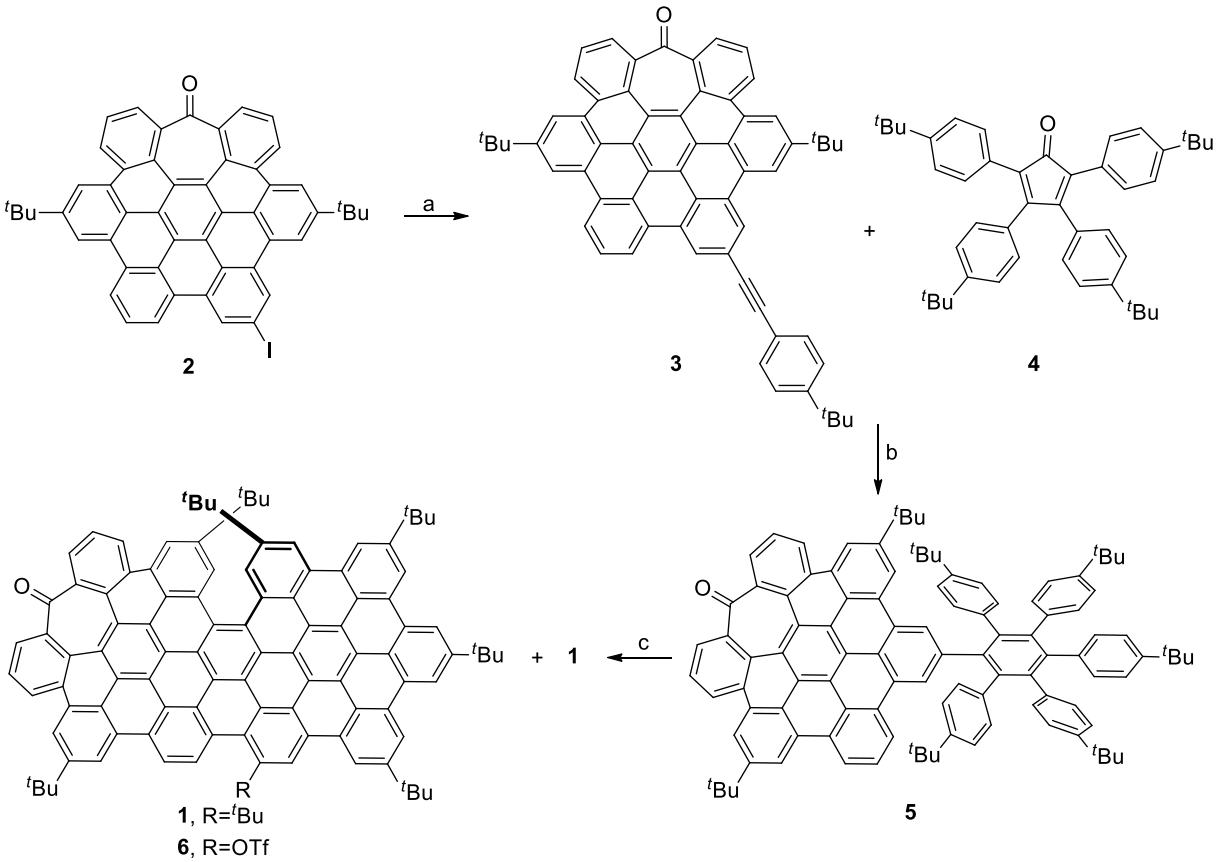

Scheme S1. Synthesis of compound **1**. Compounds **2**[S1] and **4**[S2] were prepared according to literature procedures. a) 4-*tert*-butylphenylacetylene, $PdCl_2(PPh_3)_2$, CuI, NEt_3, THF, RT, 16 h, 99%; b) Ph_2O, reflux, 8 h, 34%; c) DDQ, CF_3SO_3H, CH_2Cl_2, 0°C, 10 min, **1** (46%) and **6** (5%).

Compound 3

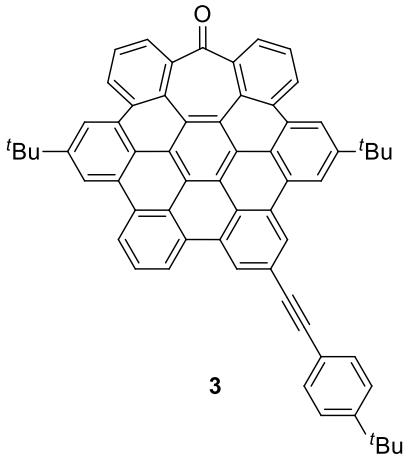

3

p-tert-Butylphenylacetylene (70 µL, 0.380 mmol) was added dropwise to a degassed suspension of **2** (100 mg, 0.127 mmol), $PdCl_2(PPh_3)_2$ (20 mg, 0.028 mmol), CuI (5 mg, 0.028 mmol) in a mixture of THF/Et_3N (1:2, 9 mL). The reaction was stirred at r.t. for 16 h. The mixture was diluted with CH_2Cl_2 (50 mL) and washed with $NH_4Cl_{(aq)}$ (2 × 50 mL) the organic layer was separated and dried over anhydrous Na_2SO_4 and the solvent was removed under reduced pressure. The crude was purified by column chromatography (SiO_2, Hexane/CH_2Cl_2 3:2) affording **3** (104 mg, 99%) as a yellow solid. M. p. > 300 ºC; ^{1}H NMR (400 MHz, CD_2Cl_2): δ = 8.75 (t, *J* = 7.6 Hz, 2H), 8.71 (s, 1H), 8.64 (m, 2H), 8.57 (s, 1H), 8.46 (s, 1H), 8.41 (d, *J* = 7.7 Hz, 1H), 8.28 (s, 1H), 8.23 (d, *J* = 8.1 Hz, 1H), 7.79 (d, *J* = 7.1 Hz, 2H), 7.67 (t, *J* = 8.0 Hz, 2H), 7.51 (t, *J* = 7.9 Hz, 1H), 7.42 – 7.34 (m, 4H), 1.66 (s, 9H), 1.57 (s, 9H), 1.37 (s, 9H); ^{13}C NMR (101 MHz, CD_2Cl_2): δ = 202.9 (C), 152.3 (C), 150.5 (C), 150.3 (C), 142.9 (C), 142.9 (C), 131.9(CH), 131.7 (C), 131.6 (C), 130.6 (C), 130.3 (C), 129.9 (C), 129.7 (C), 129.3 (C), 129.2 (C), 128.6 (C), 128.6 (C), 127.8 (CH), 127.6 (C), 127.4 (CH), 126.6 (CH), 125.9 (CH), 125.3 (C), 125.1 (C), 124.6 (CH), 124.40 (C), 124.37 (CH), 124.3 (CH), 124.0 (C), 123.6 (C), 123.35 (C), 123.34 (C), 123.2 (C), 122.3 (CH), 122.2 (C), 121.7 (CH), 121.4 (CH), 121.3 (C), 120.9 (CH), 120.7 (C), 120.5 (C), 119.0 (CH), 118.8 (C) , 90.9 (C), 89.9 (C), 36.1 (C), 36.0 (C), 35.3 (C), 32.2 (CH_3), 32.1 (CH_3), 31.6 (CH_3); HR-MS (MALDI DCTB+PPG790): *m/z* calcd. for $C_{63}H_{46}O$ $[M]^+$: 818.3543; found: 818.3559; IR (ATR): 2953, 1679, 1610, 1578 cm^{-1}.

Compound 5

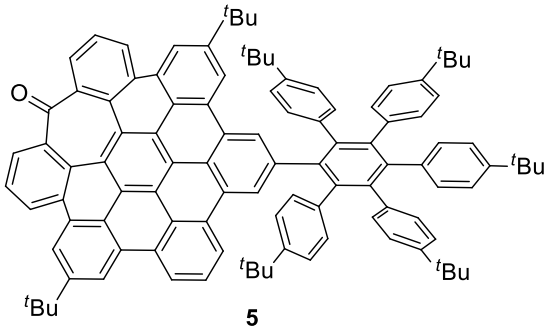

5

An equimolar amount of **3** (119 mg, 0.145 mmol) and 2,3,4,5-tetrakis(4-*tert*-butylphenyl)cyclopenta-2,4-diene-1-one (**4**) (89 mg, 0.145 mmol) were placed in a Schlenk tube, dissolved in diphenyl ether (1 mL) and bubbled with Ar. The reaction mixture was placed in a sand bath and refluxed over 8 h. The crude was allowed to cool to room temperature and diluted with CH_2Cl_2 (10 mL) and purified by column chromatography (SiO_2, Hexane/CH_2Cl_2 3:2) to afford **5** (67 mg, 33%) as a glassy yellow solid. ^{1}H NMR (500 MHz, CD_2Cl_2) δ = 9.04 (d, *J* = 8.6 Hz, 1H), 9.01 (d, *J* = 8.3 Hz, 1H), 8.90 – 8.83 (m, 4H), 8.61 – 8.57 (m, 2H), 8.50 (s, 1H), 8.43 (d, *J* = 1.4 Hz, 1H), 8.07 (t, *J* = 7.9 Hz, 1H), 7.90 (dt, *J* = 15.9, 7.6 Hz, 2H), 7.85 (dd, *J* = 7.1, 1.4 Hz, 1H), 7.82 (dd, *J* = 7.2, 1.4 Hz, 1H),

7.01 (d, J = 8.1 Hz, 2H), 6.98 – 6.91 (m, 8H), 6.90 – 6.80 (m, 8H), 6.74 (d, J = 8.2 Hz, 2H), 1.64 (s, 9H), 1.64 (s, 9H), 1.16 (s, 9H), 1.14 (s, 18H), 0.68 (s, 18H); ^{13}C NMR (126 MHz, CD_2Cl_2) δ = 202.8 (C), 150.7 (C), 150.5 (C), 148.6 (C), 148.45 (C), 148.40 (C), 142.94 (C), 142.91 (C), 141.8 (C), 141.4 (C), 141.2 (C), 140.6 (C), 140.5 (C), 138.5 (C), 138.43 (C), 138.39 (C), 131.84 (C), 131.83 (CH), 131.7 (C), 131.51 (CH), 131.48 (CH), 131.4 (CH), 130.64, 130.58 (C), 130.10 (C), 130.07 (C), 129.2 (C), 128.9 (C), 128.6 (C), 128.5 (C), 127.9 (CH), 127.8 (C), 127.7 (C), 127.6 (CH), 127.1 (CH), 126.8 (CH), 126.6 (CH), 126.4 (CH), 125.0 (C), 124.8 (C), 124.1 (CH), 124.0 (CH), 123.96 (CH), 123.75 (C), 123.73 (CH), 123.70 (CH), 123.5 (C), 123.41 (C), 123.40 (C), 122.2 (CH), 122.15 (CH), 122.12 (C), 121.5 (C), 121.4 (CH), 121.2 (C), 121.0 (CH), 118.6 (CH), 118.4 (CH), 35.9 (C), 35.9 (C), 34.4 (C), 34.2 (C), 32.0 (CH_3), 31.9 (CH_3), 31.38 (CH_3), 31.36 (CH_3), 30.9 (CH_3). Some carbon signals could not be listed due to the overlapping observed; HR-MS (MALDI DCTB + PEGNa 1500): *m/z* calcd. for $C_{107}H_{98}O$ $[M]^+$: 1398.7612; found: 1398.7594; IR (ATR): 2958, 1682, 1612, 1511 cm^{-1}.

Compounds 1 and 6

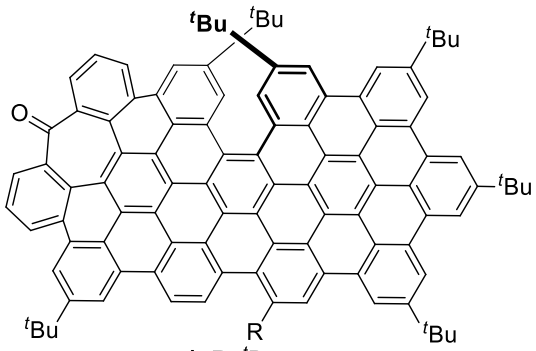

1, R=^{t}Bu
6, R=OTf

A solution of compound **5** (55 mg, 0.039 mmol) and DDQ (70 mg, 0.308 mmol) in dry CH_2Cl_2 (5 mL) was cooled to 0 – 4 ºC in an ice-water bath, then trifluoroacetic acid was added (0.1 mL, 1.306 mmol) and the mixture was stirred for 10 min. The solution was diluted with CH_2Cl_2 (3 mL), then silica gel was added and the solvent removed. The crude was purified by column chromatography (SiO_2, Hexane/CH_2Cl_2 2:8) to afford **1** (25 mg, 46%) and **6** (3 mg, 5%). **1**: M. p. > 280 ºC; $[\alpha]_D^{25}$ = -186.12º (CH_2Cl_2, c 0.037) (*M*-**1**); ^{1}H NMR (500 MHz, tetrachloroethane-d_2) δ = 10.12 (s, 1H), 9.81 (d, J = 8.1 Hz, 1H), 9.71 (d, J = 9.5 Hz, 1H), 9.70 (s, 1H), 9.66 (s, 1H), 9.60 (s, 1H), 9.56 (s, 1H), 9.52 (s, 1H), 9.49 – 9.45 (m, 3H), 9.33 (s, 1H), 9.31 (d, J = 8.3 Hz, 1H), 9.23 – 9.20 (m, 2H), 9.11 (s, 1H), 8.83 (s, 1H), 8.19 (d, J = 7.2 Hz, 1H), 8.17 – 8.12 (m, 2H), 8.10 (d, J = 7.4 Hz, 1H), 2.06 (s, 9H), 2.00 (s, 9H), 1.94 (s, 9H), 1.92 (s, 9H), 1.84 (s, 9H), 1.47 (s, 9H), 1.28 (s, 9H); ^{13}C NMR (126 MHz, CD_2Cl_2) δ = 202.7 (C), 150.53 (C), 150.3 (C), 148.9 (C), 143.5 (C), 143.2 (C), 132.5 (C), 132.2 (C), 131.5 (C), 131.3 (C), 131.2 (C), 130.8 (C), 130.0 (C), 129.4 (C), 129.3 (C), 129.3 (C), 129.2 (C), 129.0 (C), 128.7 (C), 128.59 (CH), 128.55 (CH), 128.3 (C) , 128.22 (CH), 128.19 (CH), 128.04 (CH), 128.02 (C) 127.99 (CH), 127.9 (C), 127.7 (C), 126.9 (CH), 126.3 (C), 126.1 (C), 125.9 (C), 125.63 (C), 125.58 (CH), 125.3 (C), 124.6 (C), 124.5 (C), 124.2 (CH), 124.1 (C), 123.93 (C), 123.87 (C), 123.8 (C), 123.5 (C), 123.3 (C), 122.3 (C), 121.5 (C), 121.43 (C), 121.2 (C), 120.9 (CH), 120.7 (C), 120.5 (C), 120.10 (C), 119.9 (CH), 119.81 (C), 119.79 (CH), 119.3 (CH), 118.7 (CH), 117.6 (CH), 39.9 (C), 36.3 (C), 36.2 (C), 35.8 (C), 35.52 (CH_3), 35.46 (C), 32.4 (CH_3), 32.3 (CH_3), 32.15 (CH_3), 32.12 (CH_3), 31.9 (CH_3), 31.6 (CH_3). Some carbon signals could not be listed due to the overlapping observed; HR-MS (MALDI DCTB+PPG1000+2000): *m/z* calcd. for $C_{107}H_{84}O$ $[M]^+$: 1384.6517; found: 1384.6476; IR (ATR): 2953, 1668, 1606, 1462, 1362 cm^{-1}. **6**: ^{19}F NMR (377 MHz, $(CDCl_2)_2$) δ = -75.19; HR-MS (MALDI DCTB+PMMANa 2100 + NaI): *m/z* calcd. for $C_{103}H_{75}O_2^+$ $[M - SO_2CF_3]^+$: 1343.5762; found: 1343.5745; IR (ATR): 2953, 1679, 1605, 1460, 1424 cm^{-1}.

^{1}H and ^{13}C NMR spectra of new compounds

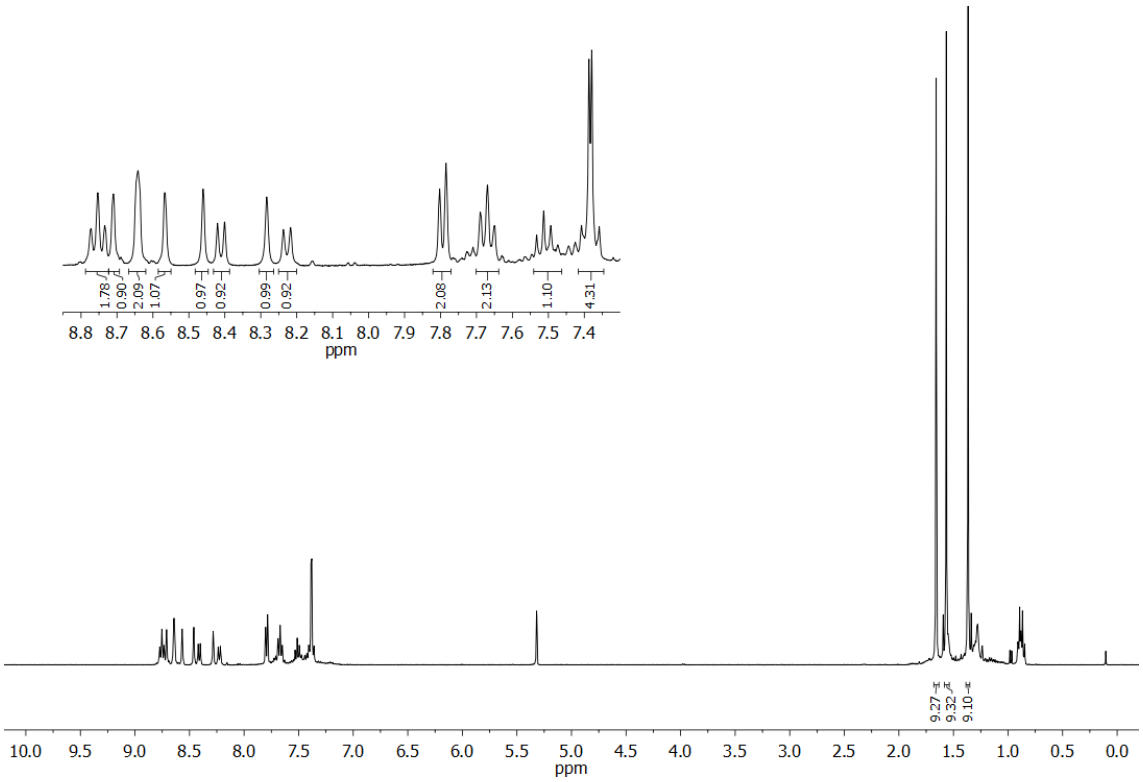

Figure S1. ^{1}H NMR (400 MHz, CD_2Cl_2) spectrum of compound **3**.

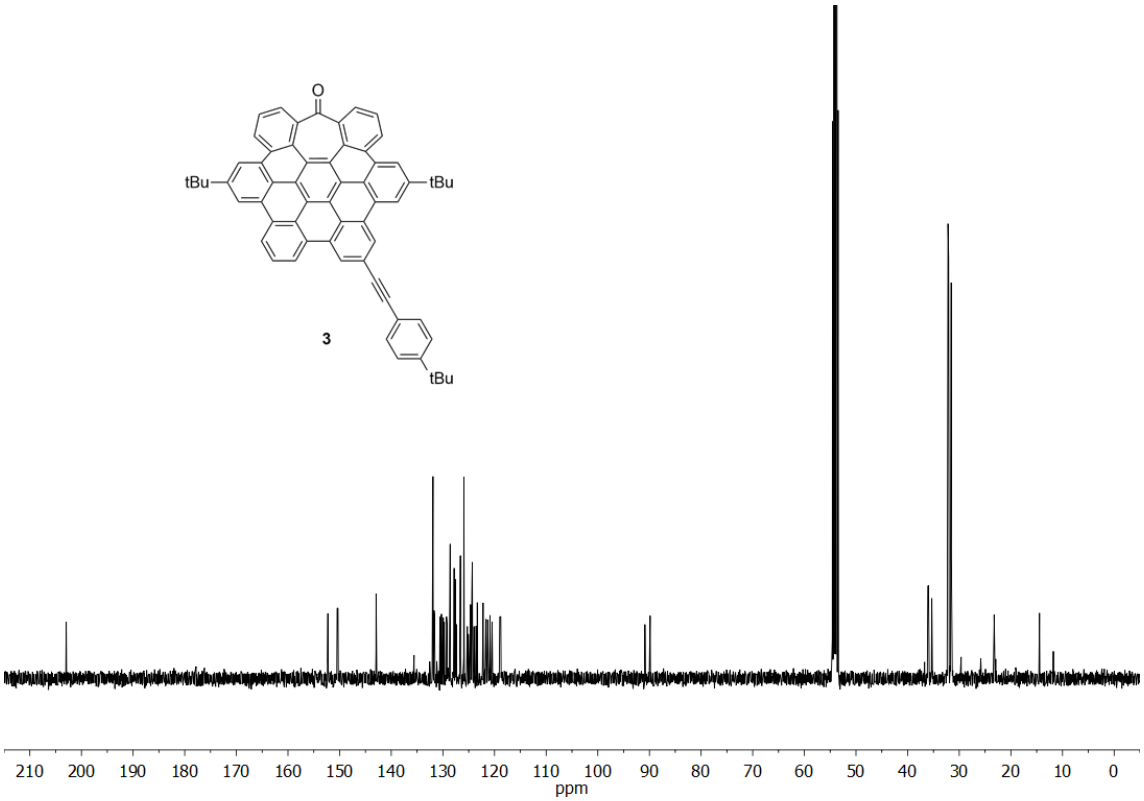

Figure S2. ^{13}C NMR (101 MHz, CD_2Cl_2) spectrum of compound **3** with residual hexane.

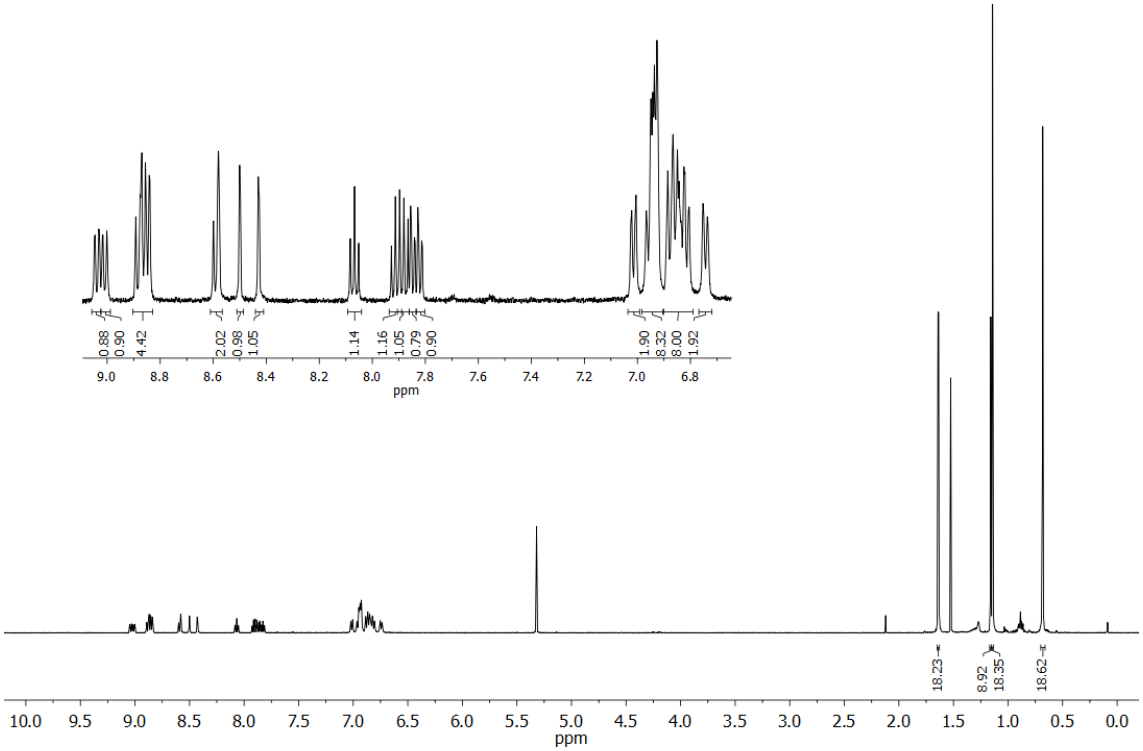

Figure S3. ^{1}H NMR (500 MHz, CD_2Cl_2) spectrum of compound **5**.

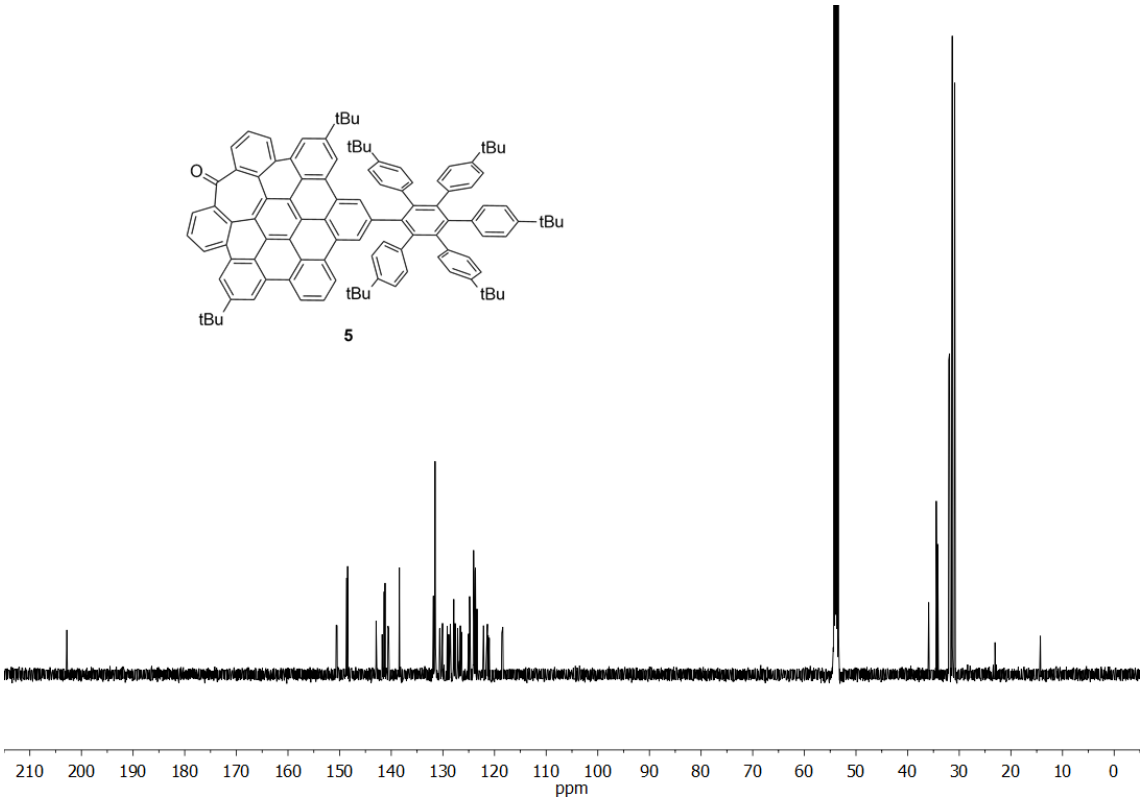

Figure S4. ^{13}C NMR (126 MHz, CD_2Cl_2) spectrum of compound **5** with residual hexane**.**

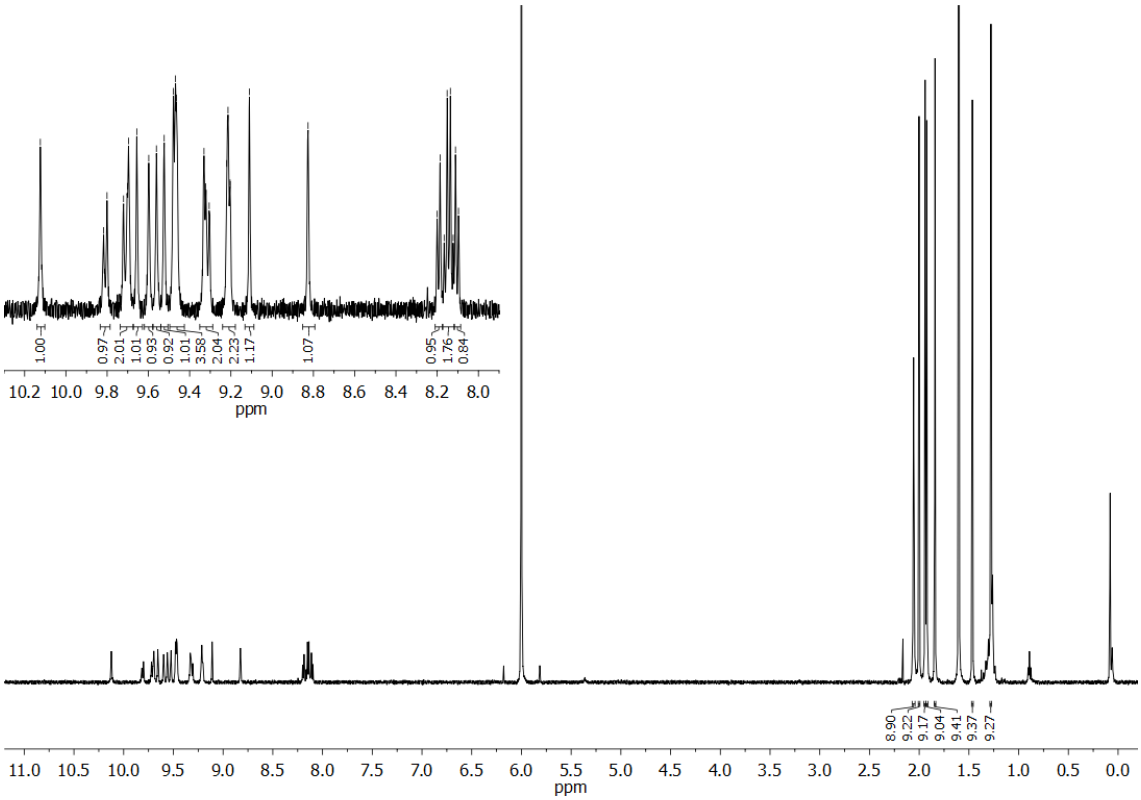

Figure S5. ^{1}H NMR (500 MHz, tetrachloroethane-d_2) spectrum of compound **1**.

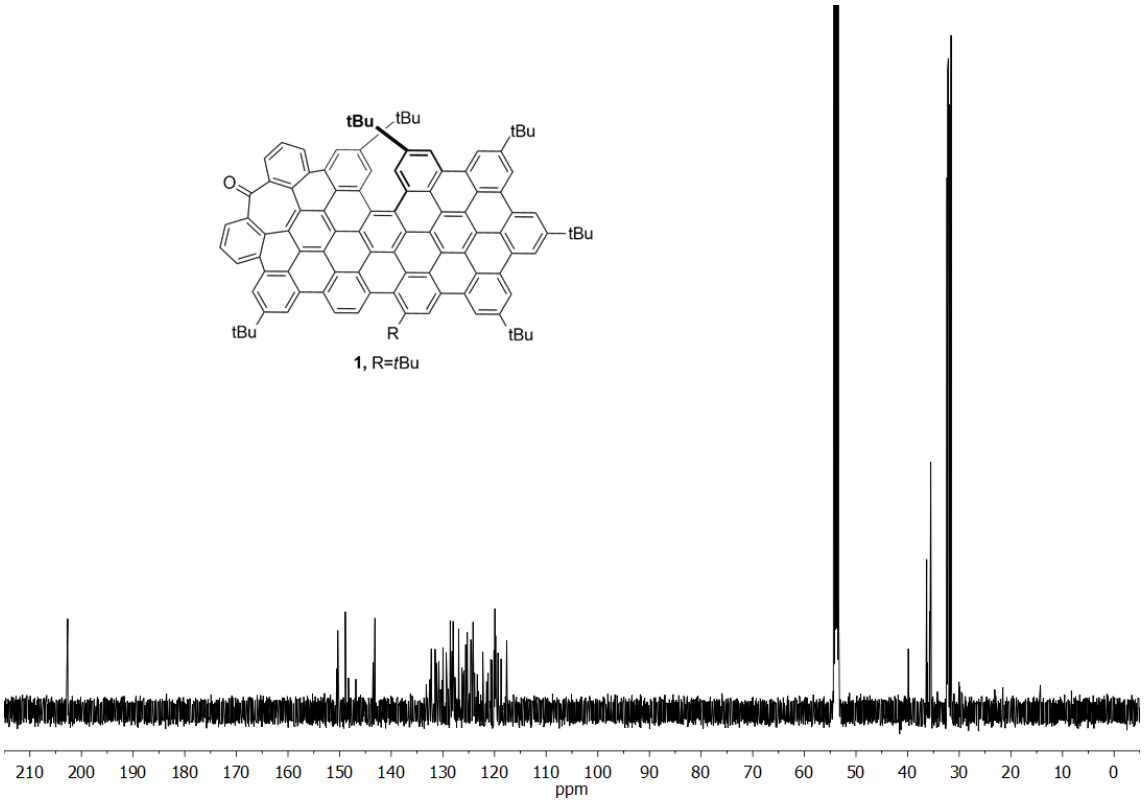

Figure S6. ^{13}C NMR (126 MHz, CD_2Cl_2) spectrum of compound **1**.

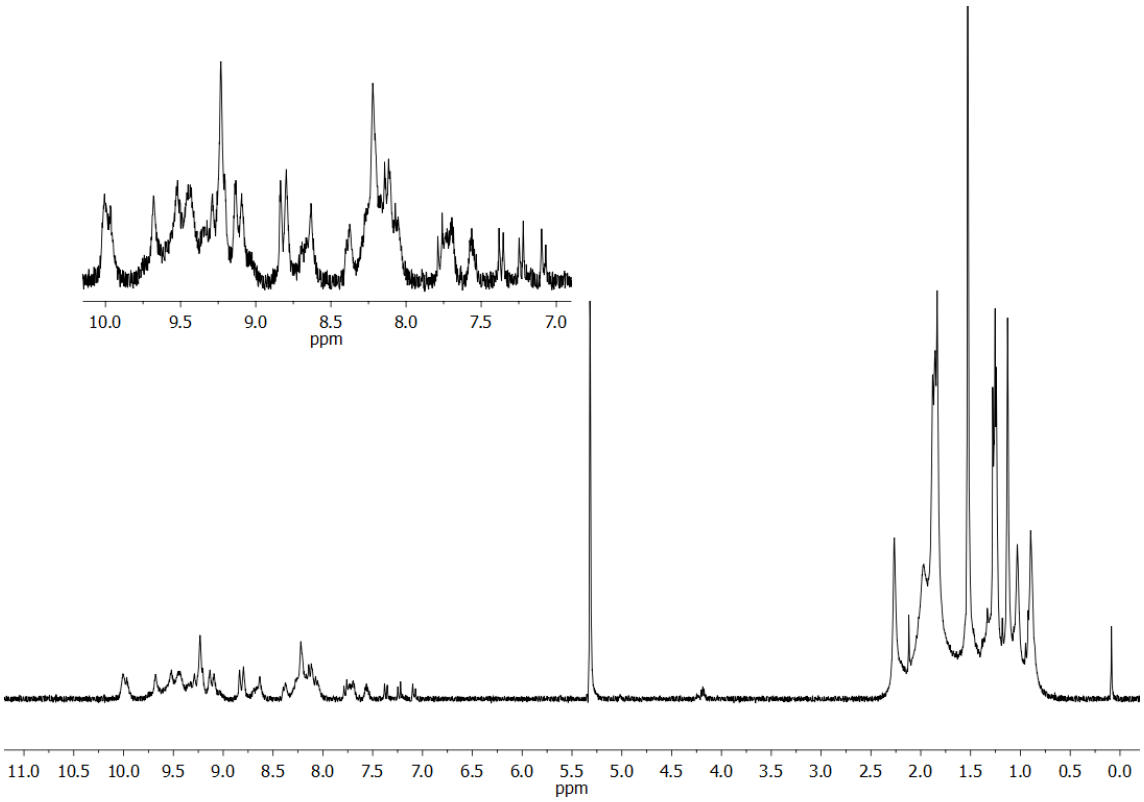

Figure S7. ^{1}H NMR (300 MHz, CD_2Cl_2) spectrum of compound **6**.

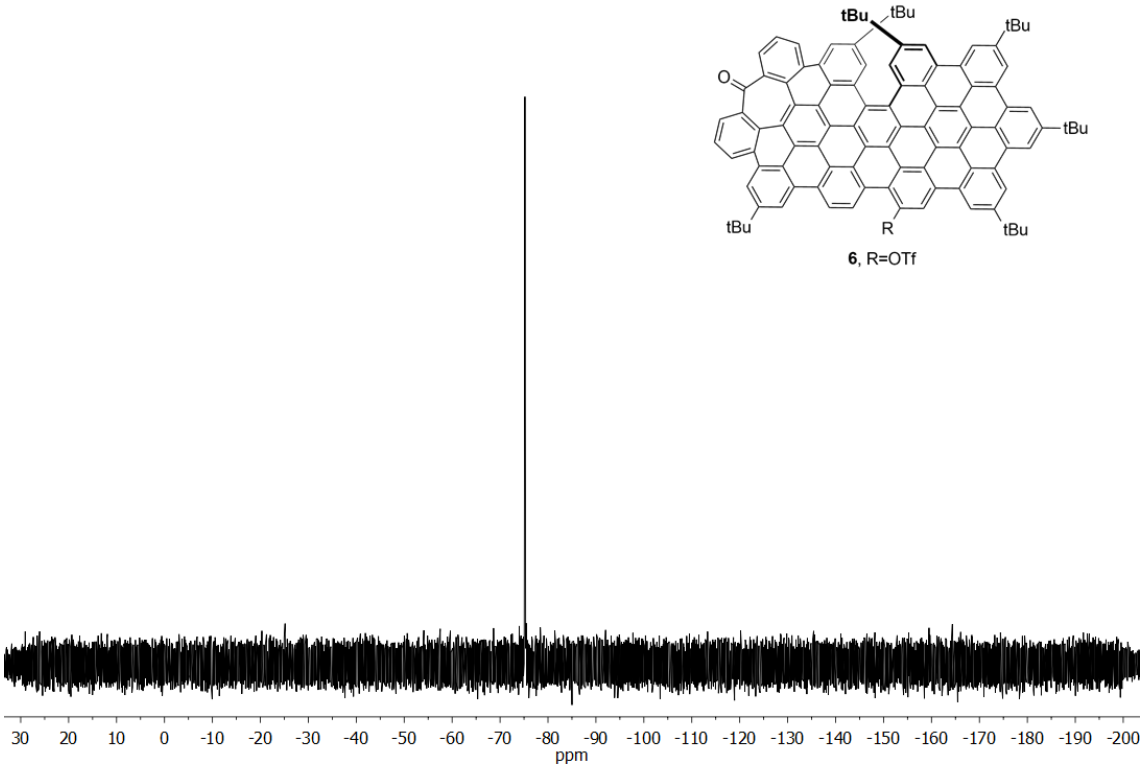

Figure S8. ^{19}F NMR (377 MHz, tetrachloroethane-d_2) spectrum of compound **6**.

2D-NMR, VT-NMR, MALDI-HRMS and IR spectra of compound 1

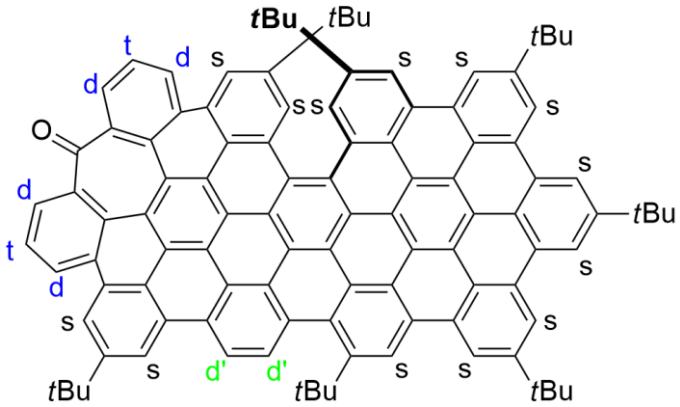

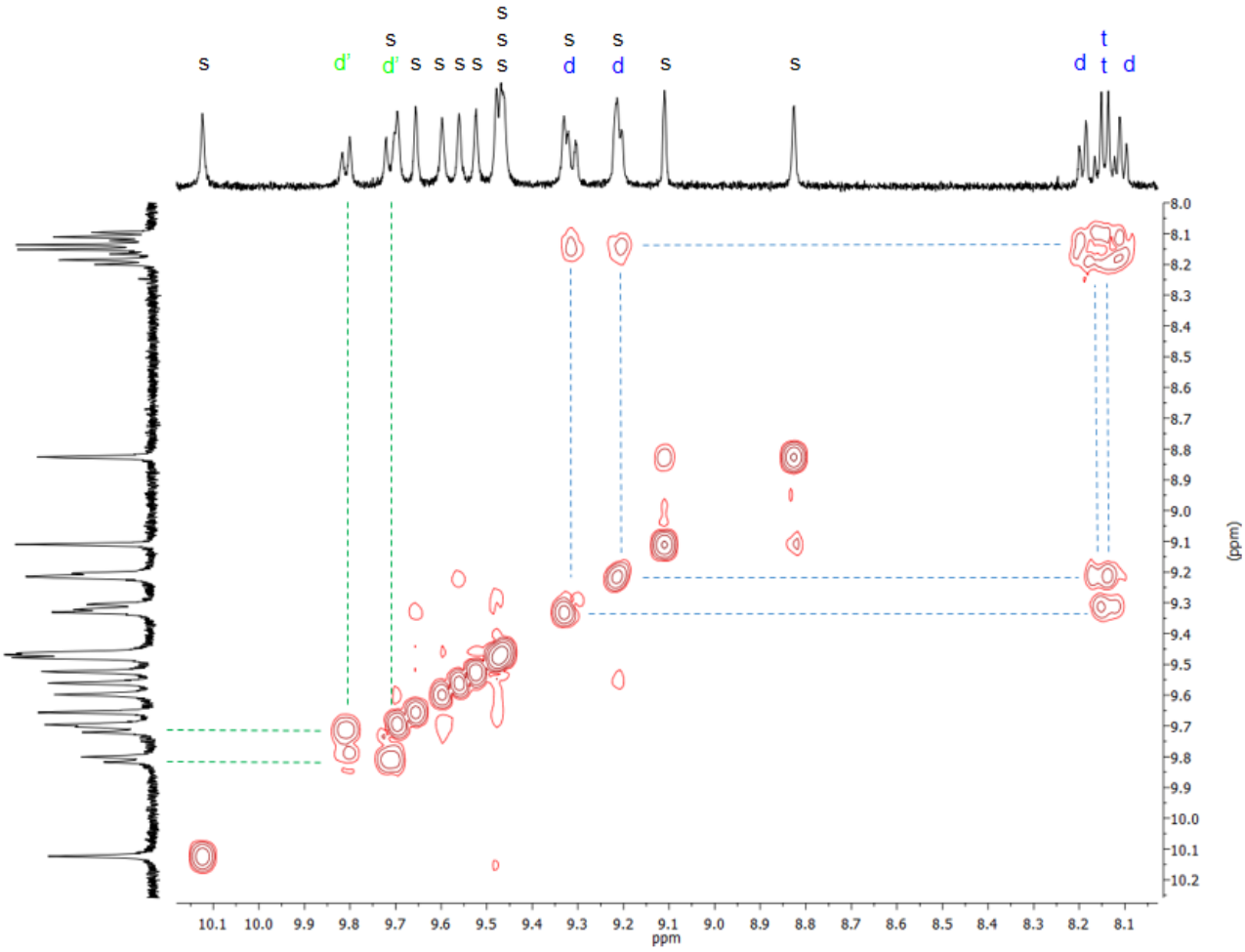

Figure S9. Partial ^{1}H-COSY (500 MHz, tetrachloroethane-d_2) spectrum of compound **1**.

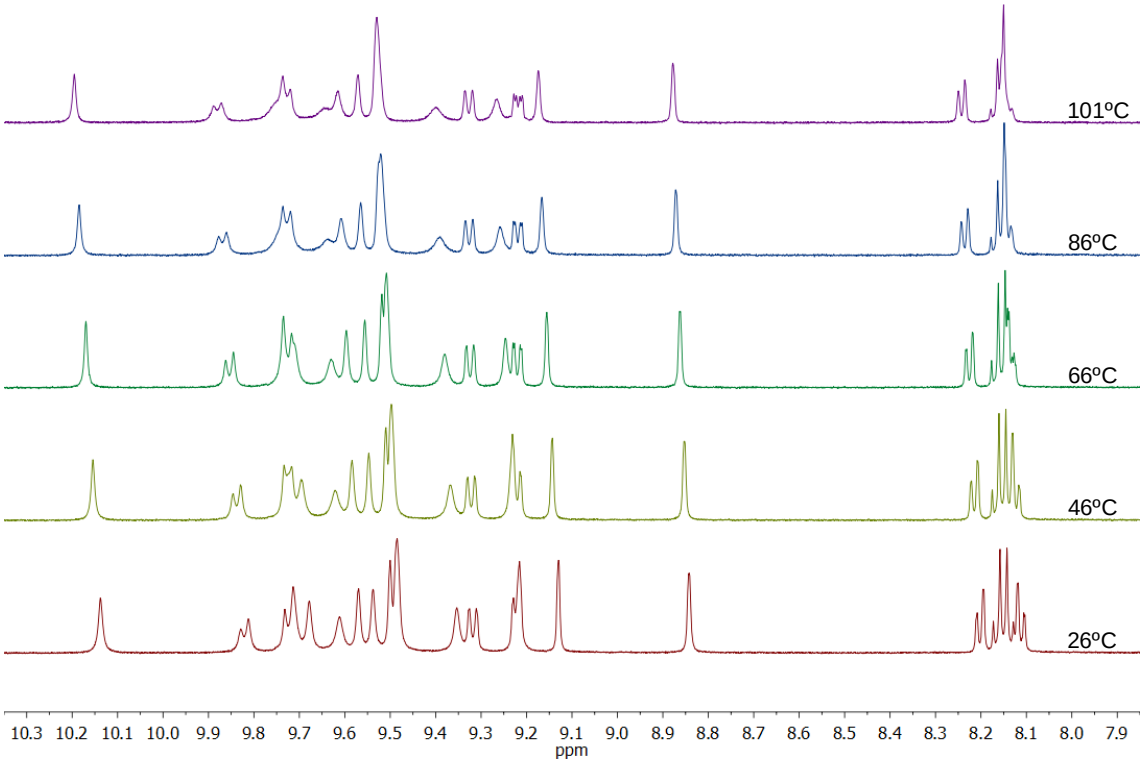

Figure S10. Partial VT ^{1}H NMR (500 MHz, tetrachloroethane-d_2) spectra of compound **1**.

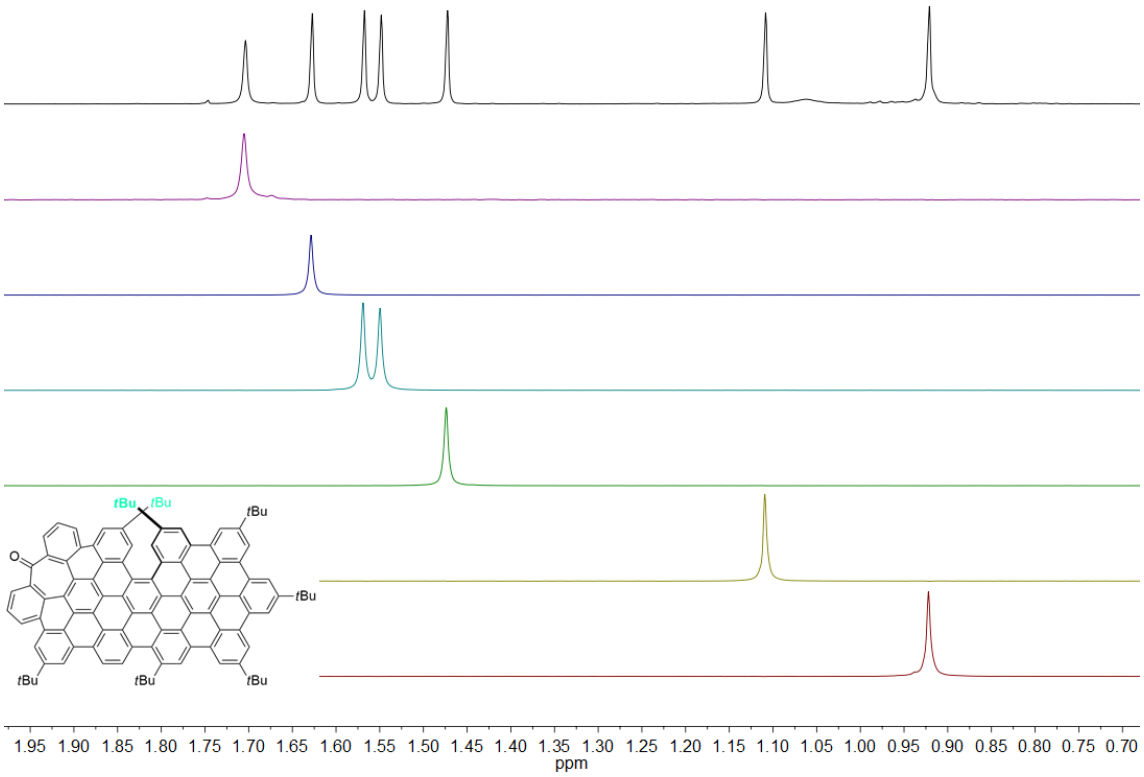

Figure S11. Partial NOESY-1D ^{1}H NMR (500 MHz, tetrachloroethane-d_2) spectra of compound **1** at 101ºC showing the nOe response when irradiating each of the *t*Bu groups. As expected nOe effect was only observed between two of the *t*Bu groups (pale blue spectrum), which should correspond to those located on the [5]helicene moiety. Black spectrum correspond to the *t*Bu zone of the ^{1}H NMR spectrum.

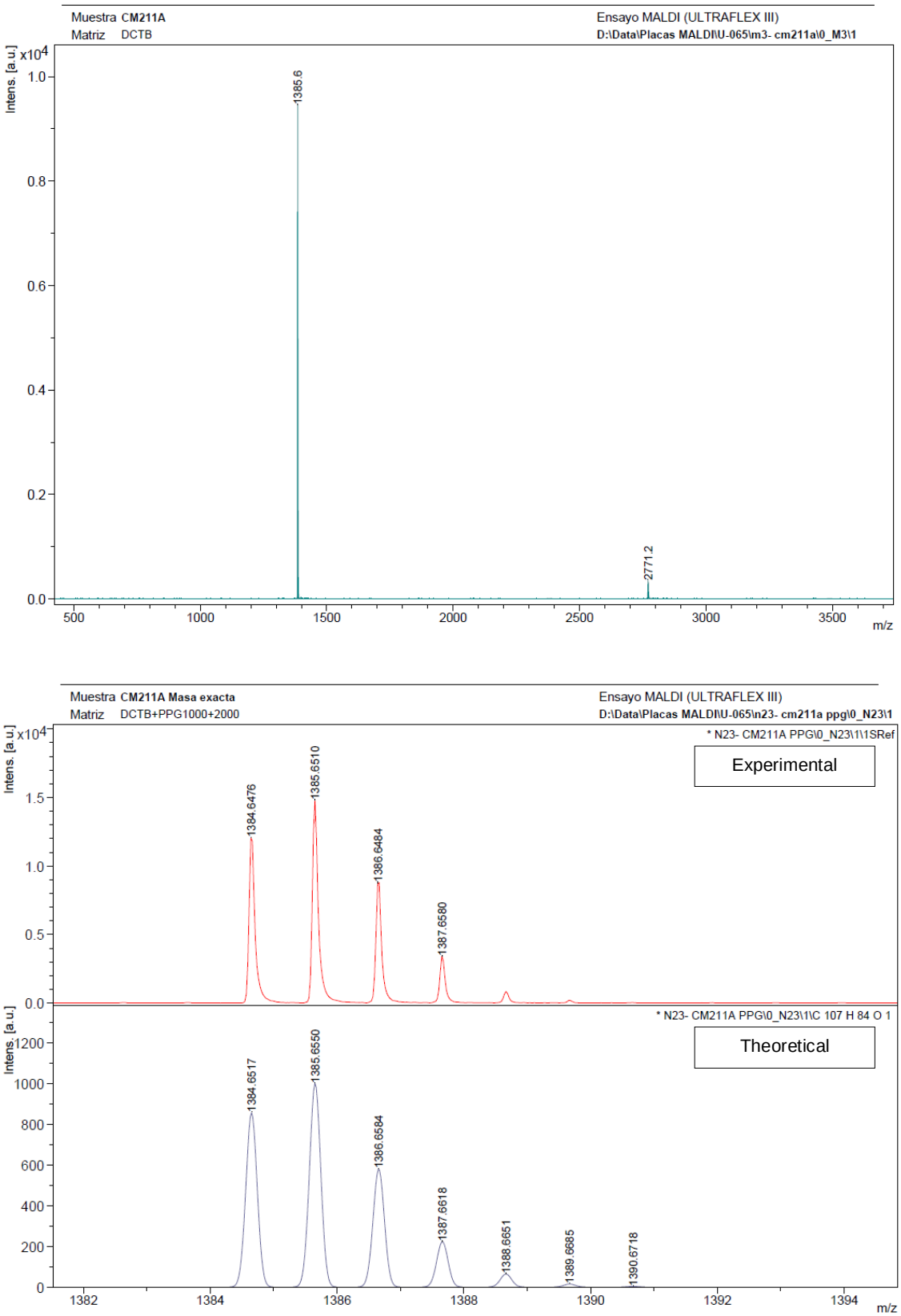

Figure S12. MS (MALDI-TOF) (top) and HR-MS (MALDI-TOF) (bottom) spectra of compound **1**.

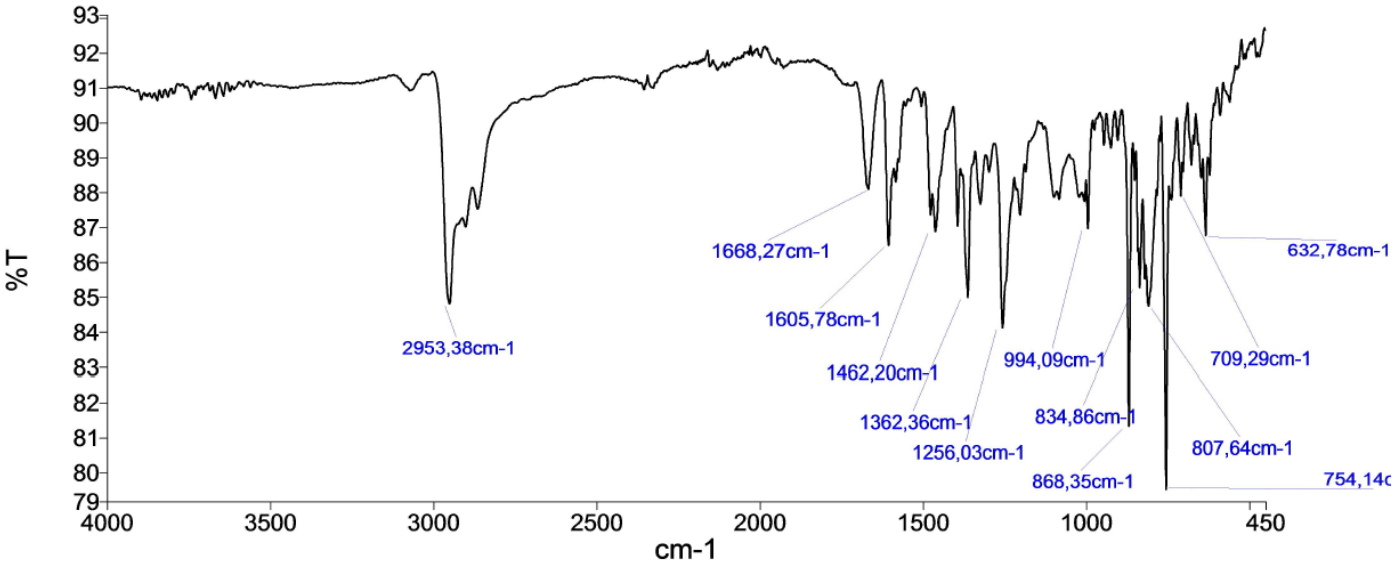

Figure S13. IR spectrum of compound **1**.

HPLC Traces

Racemic resolution of *M* and *P* enantiomers of compound **1** was carried out on an *Agilent* 1260 series equipped with the following modules: quaternary pump (G7111B 1260 Quat Pump), automatic sample injector (G2258A 1260 DL ALS), column thermostat (G1316A 1260 TCC), DAD detector (G7115A 1260 DADWR) and an automatic sample collector (G1364C 1260 FC-AS).

Analytical methodology

For analytical assays, CHIRALPAK® IC analytical column packed with cellulose *tris*-(3,5-dichlorophenylcarbamate) immobilized on silica gel (5µm) was used. The column temperature was set at 25 °C and the flow was constant during operation (0.6 mL/min). The mobile phase gradient used is shown on Table S1. 444 nm was selected as reference wavelength for the peak detection.

Table S1. Mobile phase gradient used for analytical racemic resolution of compound **1**

Time (min)	Hexane (%)	CH_2Cl_2 (%)
5.00	80.0	20.0
10.00	70.0	30.0
15.00	60.0	40.0
20.00	50.0	50.0
25.00	40.0	60.0
30.00	30.0	70.0
35.00	20.0	80.0
37.00	30.0	70.0
39.00	40.0	60.0
40.00	50.0	50.0
42.00	80.0	20.0

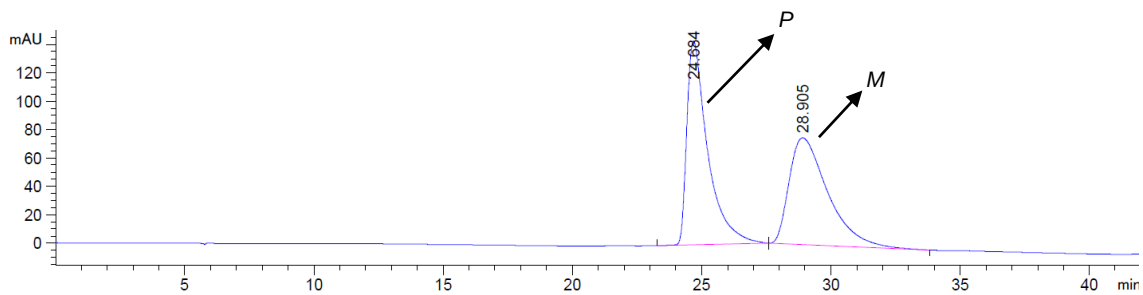

Peak #	RetTime [min]	Type	Width [min]	Area [mAU*s]	Height [mAU]	Area %
1	24.684	BB	0.8224	8060.93213	143.71843	50.7154
2	28.905	BB	1.5136	7833.51367	75.30316	49.2846
Totals :				1.58944e4	219.02159	

Figure S14. Chromatogram and peak information for the separation of *P*-**1** and *M*-**1** after the analytical run.

Semipreparative methodology

For semipreparative assays, CHIRALPAK® IC semipreparative column packed with cellulose *tris*-(3,5-dichlorophenylcarbamate) immobilized on silica-gel (5µm) was used. The column temperature was set at 25 °C and the flow was constant during operation (3.8 mL/min). The mobile phase gradient used is shown on Table S2. 510 nm was selected as reference wavelength for the peak detection.

Table S2. Mobile phase gradient used for semipreparative racemic resolution of compound **1**

Time (min)	Hexane (%)	CH_2Cl_2 (%)
2.50	80.0	20.0
5.00	70.0	30.0
7.50	60.0	40.0
10.00	50.0	50.0
12.50	40.0	60.0
14.00	60.0	40.0
15.00	80.0	20.0
16.00	80.0	20.0

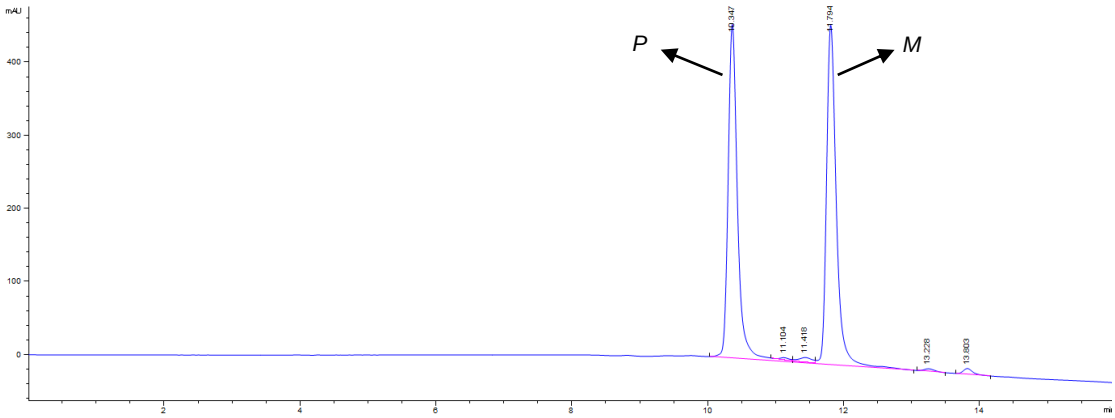

Peak #	RetTime [min]	Type	Width [min]	Area [mAU*s]	Height [mAU]	Area %
1	10.347	BV R	0.1441	4387.86670	456.74200	47.3728
2	11.104	VV E	0.1574	35.65257	3.26486	0.3849
3	11.418	VV E	0.1998	95.10860	6.69242	1.0268
4	11.794	VB	0.1523	4632.26221	464.69196	50.0114
5	13.228	BB	0.1657	37.10987	3.44412	0.4007
6	13.803	BBA	0.1455	74.41241	7.78450	0.8034
Totals :				9262.41237	942.61986	

Figure S15. Chromatogram and peak information for the separation of *P*-**1** and *M*-**1** after the semipreparative run.

Racemization studies

For racemization studies three solutions of enantiopure compound **1** (1 mg/mL) in hexadecane (3 mL) were heated at three different temperatures (140, 160 and 180°C) taking aliquots every 10 min (140 °C) or 5 min (160 ºC and 180 °C). These aliquots were analyzed by chiral HPLC in order to determine its enantiomeric excess.

Ln(ee%) values were plotted versus time and the data set for each temperature was fitted to a first order kinetic equation (1) determining the racemization rate at each temperature (k(T)) as: k(413K) = 2×10^{-5} s^{-1}, k(433K) = 1×10^{-4} s^{-1} and k(453K) = 7×10^{-4} s^{-1} (Figure S16).

The values of $\Delta H^{\ddagger}$ and $\Delta S^{\ddagger}$ of racemization could be obtained from rate constants k(T) values using an extended version of the Eyring-Polanyi equation (2). $\Delta G^{\ddagger}$ (298K) was therefore estimated as 32.994 kcal mol^{-1}.

$$\ln(ee) = -k \cdot t \tag{1}$$

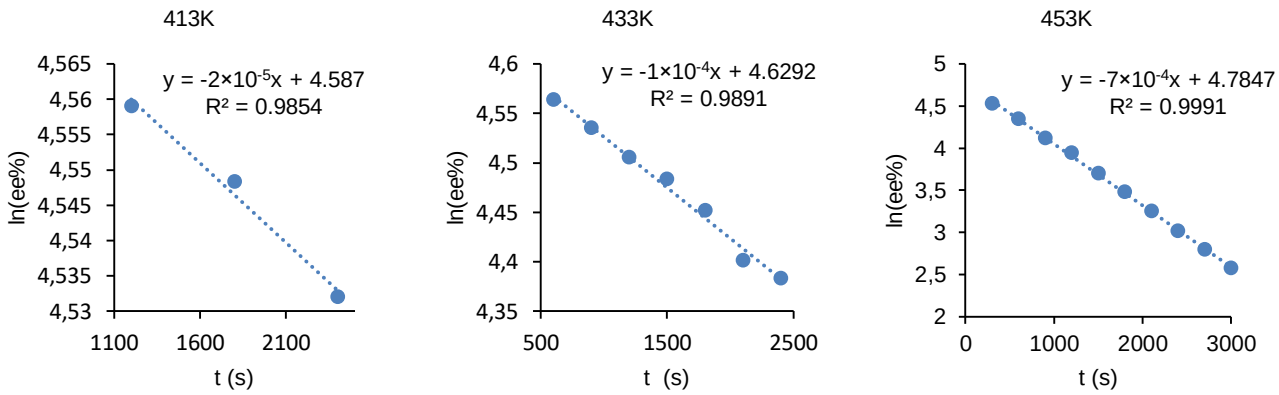

Figure S16. Plots of ln(ee%) vs time at three different temperatures.

$$\ln\left(\frac{k}{T}\right) = \frac{-\Delta H^{\ddagger}}{R} \cdot \frac{1}{T} + ln\frac{k_B}{h} + \frac{\Delta S^{\ddagger}}{R} \tag{2}$$

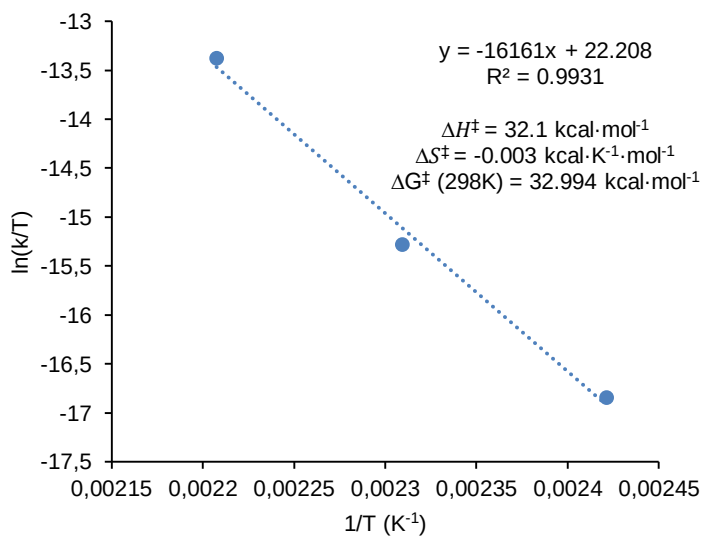

Figure S17. Eyring-Polanyi plot

Photophysical properties of 1

The linear absorption spectra were recorded in a JASCO V-540 spectrophotometer. The fluorescence spectra were recorded using a Horiba Jobin Yvon Fluorlog 3-22 Spectrofluorimeter with a xenon lamp of 450 W. The spectra were recorded at μM concentrations in spectroscopic grade solvents. The fluorescence quantum yields were determined using Fluorescein in 0.1M NaOH as standard. The TPA spectra were measured by two-photon fluorescence (TPF) using Rhodamine 6G in methanol as standard to account for the collection efficiency and excitation pulse characteristics.[S3] The excitation source was a Ti:sapphire laser (Tsunami BB, Spectra-Physics, 710-990 nm, 1.7 W, 100 fs, 82 MHz). A modified setup that follows the one described by Xu and Webb was used to estimate the TPA cross-section in the 710-990 nm region.[S4] The two-photon absorption cross-section was calculated from the equation:

$$\sigma_2 = \left(\frac{F_2}{\phi C n}\right)_s \left(\frac{\phi C n \sigma_2}{F_2}\right)_{ref} \tag{3}$$

where F_2 stands for two-photon induced fluorescence intensity, ϕ is the one-photon excited fluorescence quantum yield, n refers to the refractive index in solution, C is the concentration and s and ref are relative to the sample and the TPA reference, respectively. The emission intensity dependence of the excitation power was checked to be quadratic.The two-photon emission was measured within a narrow wavelength bandwidth selected by the H20Vis Jobin Yvon monochromator placed at the entrance of a PMC-100-4 photomultiplyer tube (Becker and Hickl GmbH). The integrated intensity over the entire emission band was extrapolated using the emission spectra corrected by the detector sensitivity. The fluorescence intensity was measured in a single photon count mode by integrating the number of emitted photon in a 10 ns time interval after the excitation pulse. This time interval is limited by the repetition rate of our excitation source and due to the long emission lifetime of compound **1** (24 ns) it is shorter than the time needed to collect all the emitted photons. To extrapolate the total number of emitted photon a correction factor was estimated from the ratio of the number of photons emitted within 10 ns to the overall number of photons emitted determined from the lifetime measured in a different setup that does allow for collection of all the emitted photons. The emission lifetimes shown in Figure S18a were measured by the Single-Photon Timing technique in a home-built setup using a linear excitation source operating at 330 nm with a 4MHz repetition rate (second harmonic of a Coherent Radiation Dye laser 700 series, 610-680 nm, 130 mW, 5 ps, 4 MHz), an Hamamatsu R2809U-01 MCP-PMT (290−700 nm) as the detector and an SPC-160 photon counting board from Becker & Hickl GmbH. The emission at 560 and 620 nm was collected at the magic angle. The instrument response functions (IRF) for deconvolution (280 ps FWHM) were generated by scattering dispersions of colloidal silica in water. The solution was kept under gentle stirring during the data collection. Blank decays were acquired to ensure that dark photon counts were negligible. Decay curves were stored in 1024 channels with 136.7 ps per channel and an accumulation of 20k counts in the peak channel. The fluorescence decays were analysed by a non-linear least-squares reconvolution method using the TRFA DP software by SSTC (Scientific Software Technologies Center, Belarusian State University, Minsk, Belarus). Recovering the species-associated emission spectra (SAEMS) for each one of the decay times was not possible due to the residual dependence of the amplitude associated with each time-constant on the emission wavelength.

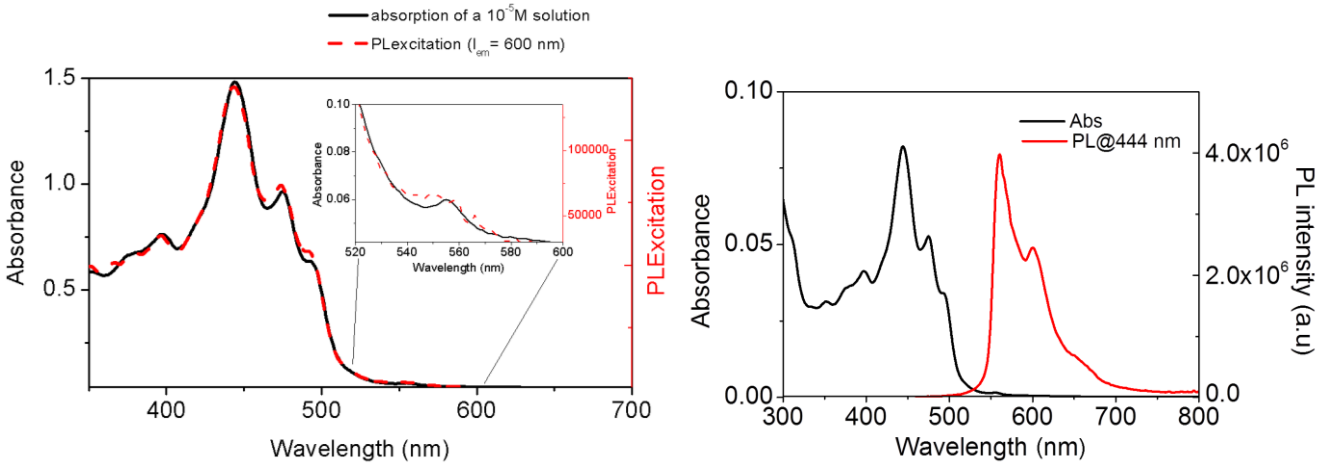

Figure S18. Left: Absorption and excitation spectra of **1** in CH_2Cl_2 recorded in the 300-700 region. Right: absorption and fluorescence emission spectra of **1** in CH_2Cl_2. Emission was collected upon excitation at the absorption maximum at 444 nm.

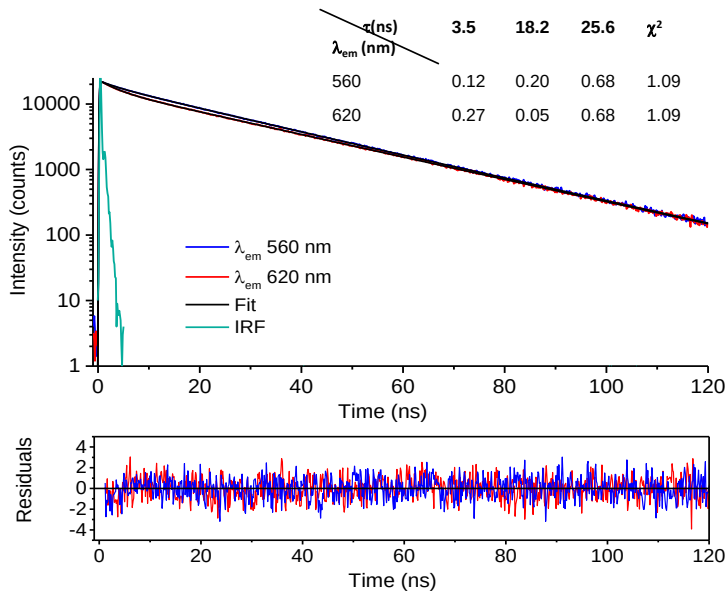

Figure S18a. Fluorescence emission decays of compound **1** in CH_2Cl_2 collected at 560 nm (in blue) and 620 nm (in red) and corresponding multiexponential fitting. The instrumental response function (IRF) is shown in green. For a better judgment of the quality of the fits, the residuals are presented and the fitting parameters are listed in the table.

Optical band gap

As commented in the manuscript, optical band gap was estimated from the curve crossing of the normalized absorption and emission spectra as 2.22 eV. The lowest energy S0→S1 transition, calculated at 527 nm (Table S5), is observed as a very weak band at 555 nm in agreement with its predicted weak oscilator strength. This band is only clearly observed in more concentrated solutions (10^{-5} M).

Electronic circular dichroism and circularly polarized luminescence measurements

Electronic circular dichroism (ECD) spectroscopy and circularly polarized luminiscence (CPL) were recorded in an Olis DSM172 spectrophotometer with a xenon lamp of 150 W. The spectra were recorded at 1×10^{-5} M concentrations in HPLC grade solvents. For ECD measurements a fixed slitwidth of 1 mm and 0.1 s of integration time were selected, the ECD spectra showed in Figure S19 are an average spectra calculated after 20 scans (each one). For CPL measurements a fixed wavelength LED (372 nm) and 1.0 s of integration time were selected, the CPL spectra showed in figure S21 are an average spectra calculated after 100 scans (each one).

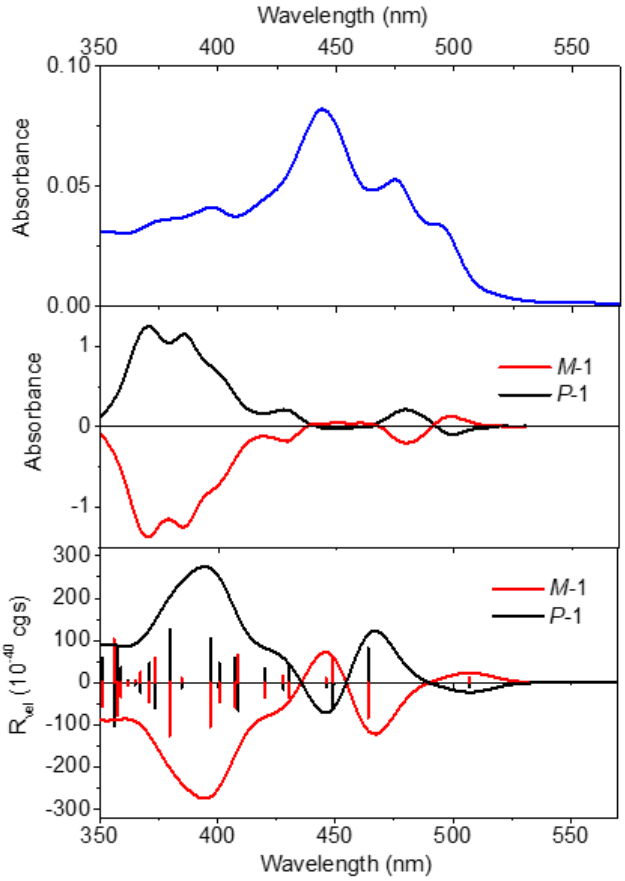

Figure S19. Absorbance spectrum of **1** (top, blue line), CD spectra of *P* (black line) and *M* (red line) enantiomers of **1** in CH_2Cl_2 at 25 ºC, both recorded at Olis DSM 172 (middle) and simulated CD spectra of *P* (black line) and *M* (red line) enantiomers of **1** (down).

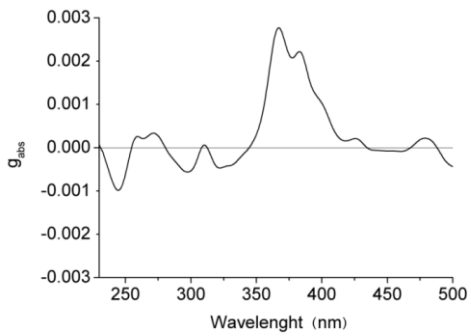

Figure S20: g_{abs} spectrum of *P*-**1**.

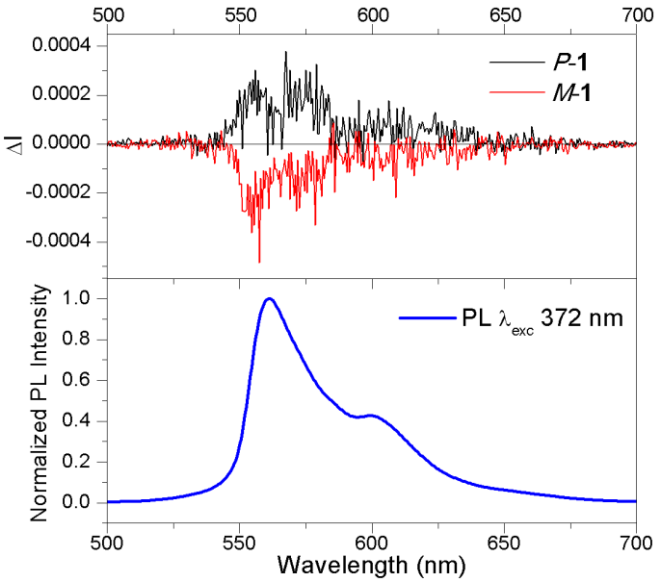

Figure S21. Normalized fluorescence spectrum of **1** (bottom, blue line) and CPL spectra of the *P* (black line) and *M* (red line) enantiomers of **1** in CH_2Cl_2 at 25 ºC (top).

Electrochemical measurements of 1

Cyclic Voltammetry (CV) and Square Wave Voltammetry (SWV) were carried out on a PGSTAT204 potentiostat/galvanostat (Metrohm Autolab B. V.) with a three electrode cell under Ar atmosphere at 25 ºC. A Pt-wire counterelectrode, an Ag-wire quasireference electrode and a glassy carbon disk working electrode were used.

Freshly distilled THF was used as solvent to prepare a 0.1 M solution of tetra-*n*-butylammonium hexafluorophosphate ($TBAPF_6$) which was used as work solution. Scan rate was 0.1 V/s. Potential values are referred to the ferrocenium/ferrocene ($FeCp_2^+/FeCp_2$) system, Fc added as an internal reference after each measurement.

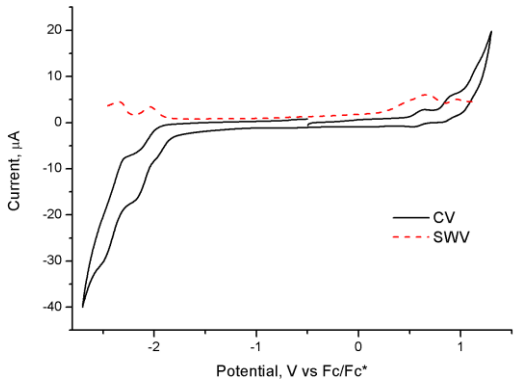

Figure S22. Cyclic (black line) and square wave (red - - -) voltammograms of **1** (4 mM) in THF (internal standard Fc/Fc^+, v = 0.1 V/s).

Spectroelectrochemical measurements of 1

Spectroelectrochemical measurements were carried out on a PGSTAT204 with an Autolab Spectrophotometer UB module on a three electrode cuvette (0.1 cm pathlenght) under Ar atmosphere at 25 ºC. A Pt-wire counterelectrode, an Ag-wire quasireference electrode and a Pt-mesh working electrode were used.

A 0.1 M solution of $TBAPF_6$ in freshly distilled THF was used as work solution. A 1 mM solution of compound **1** was measured, and the new optical active species generated were observed. Scan rate was 0.1 V/s. Spectra were recorded every 50 mV from 198 to 765 nm. During a potential sweep, the new species generated exhibited significantly red-shifted absorption maxima at 710 and 680 nm upon oxidation and reduction, respectively, drastically diminishing the optical band gaps down to 1.74 eV upon oxidation and to 1.82 eV upon reduction (in this case, the optical band gaps have been estimated at the corresponding new absorption maxima).

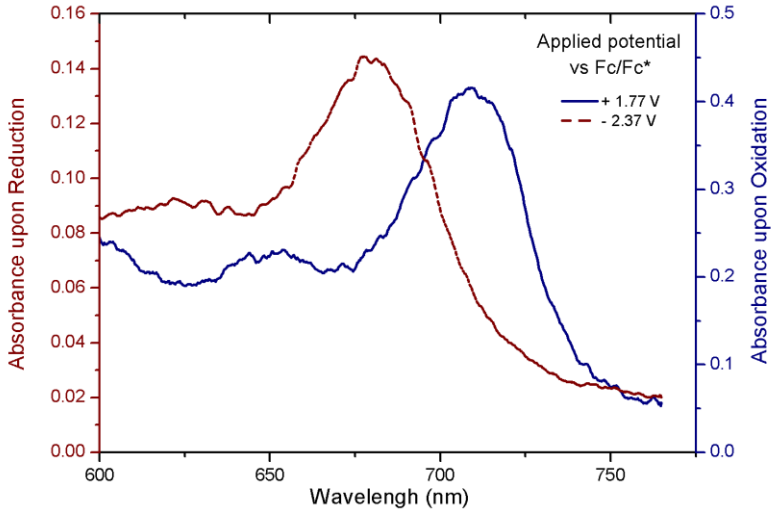

Figure S23a. UV-Vis absorbance spectrum at two selected applied potential showing the absortion maxima of the new oxidized and reduced species generated.

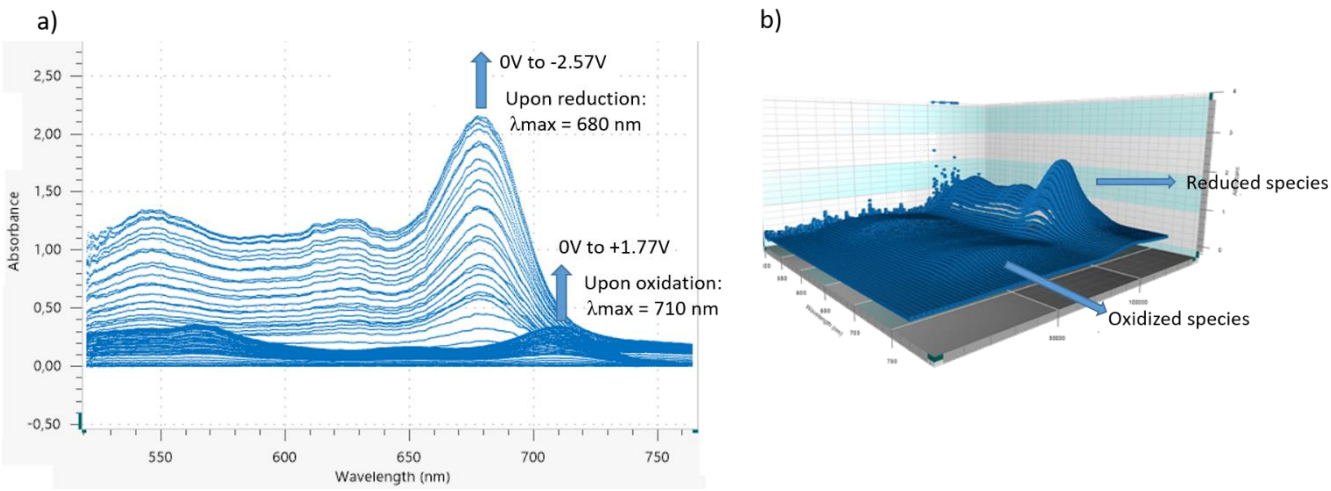

Figure S24b. UV Vis absorbance spectrum as function of current intensity in the range from 500 to 765 nm: a) 2D spectrum; b) 3D spectrum showing the absorbance spectrum after one complete scan.

Spectroscopic measurements (UV-Vis and ECD) upon addition of magic blue were recorded inn an Olis DSM172. A solution of compound **1** (1×10^{-5} M) in CH_2Cl_2 (3 mL) was prepared and then a solution of "magic blue" (15 µL, 2 mM) in CH_2Cl_2 were subsequent added. A fixed slitwidth of 1 mm and an integration time of 0.01 s for absorbance spectra and 0.1 s for ECD spectra were selected. A new absorption maxima shifted to 672 nm appears showing also a small response in ECD.

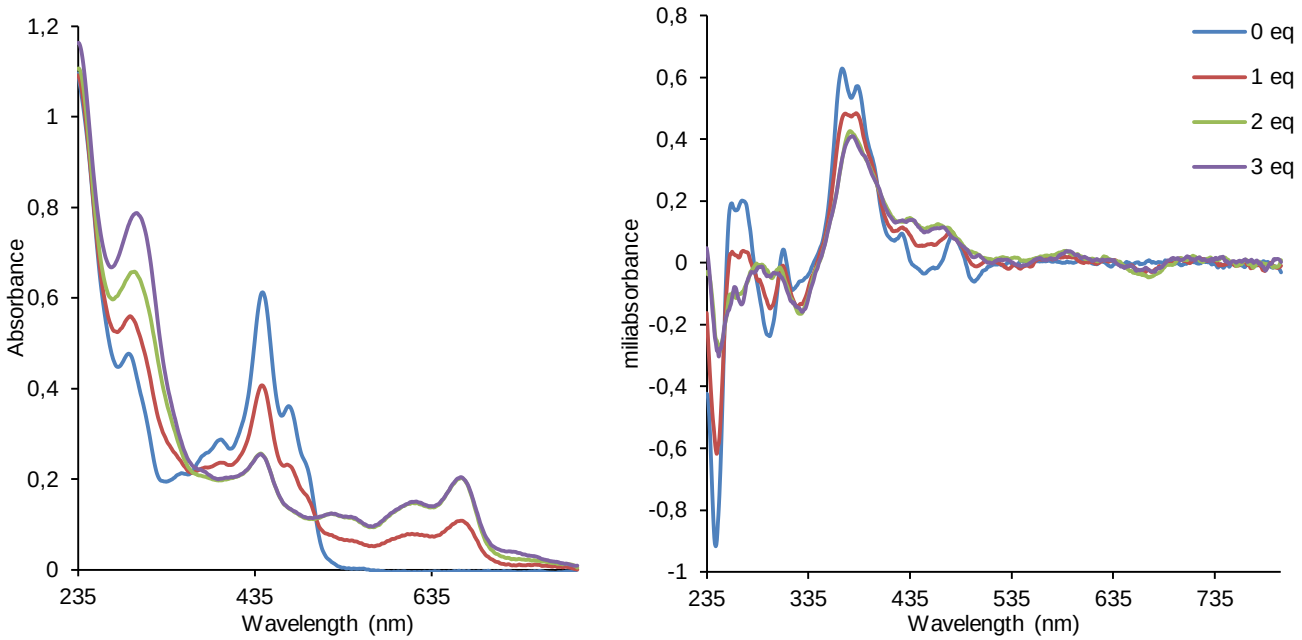

Figure S25. Absorbance (left) and ECD (right) spectra of compound **1** after subsequent additions of "magic blue".

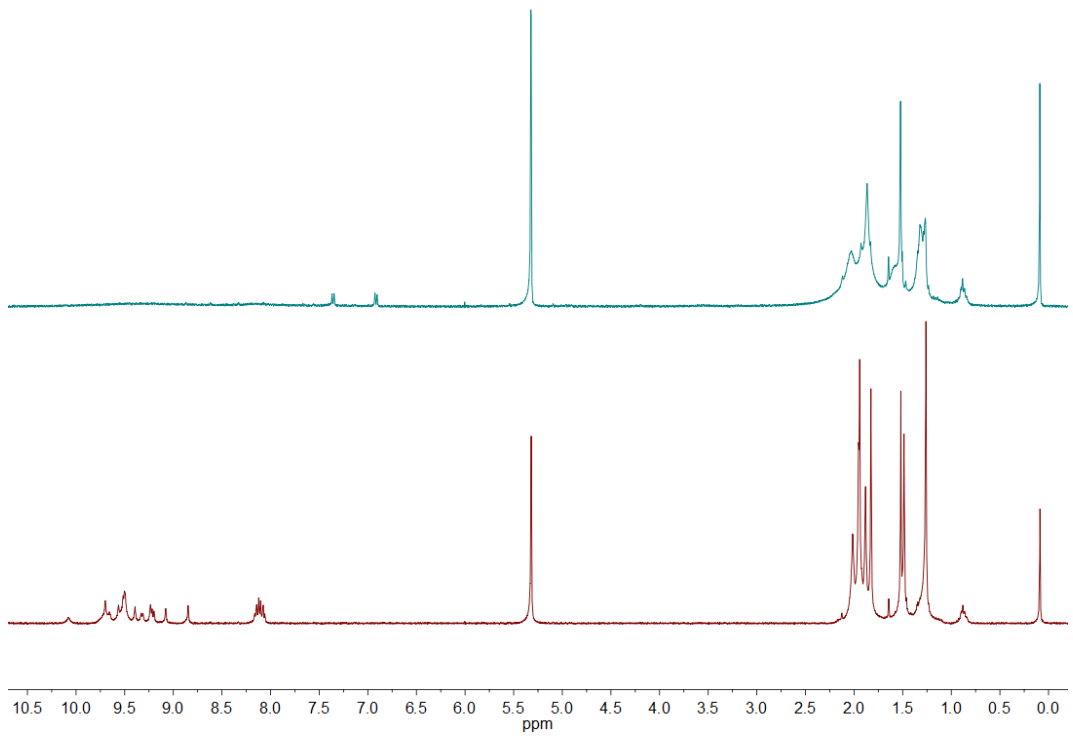

Figure S26. ^{1}H NMR (400 MHz, CD_2Cl_2) spectra of compound **1** before (bottom, red) and after addition of 1 equiv. of "magic blue" (top, blue).

Single crystal X-Ray Analysis

Single crystals suitable for X-ray diffraction crystallography of **1** were grown by slow diffusion of methanol vapor into a solution of **1** in chlorobenzene. We have also grown X-ray diffraction quality crystals of **6** by slow evaporation of a solution of the compound in a CH_2Cl_2/hexane mixture. The X-ray diffraction data were collected on a Bruker D8 Venture diffractometer equipped with a Photon 100 detector. The structures were solved with the SHELXT[S5] software (direct methods) and refined using the full-matrix least-squares against F^2 procedure with SHELX 2016[S6] using the WinGX32[S7] software. Hydrogen atoms were placed in idealized positions (U_{eg}(H) = 1.2U_{eg}(C) or U_{eg}(H) = 1.5U_{eg}(C)) and were allowed to ride on their parent atoms. A summary of the X-ray diffraction measurement and refinement data is given in Table S3. During the refinement of **1** the structure of the molecule was established unambiguously and obtained with reasonable thermal ellipsoids. However large residual electron density, located mainly in the voids between the ribbon-shaped nanographene molecules, remained present and could not be modeled. This is probably due to the presence of disordered chlorobenzene molecules that occupy that space, as other two other solvent molecules in the assymetric unit that could be modelled were present in the structure. To tackle this issue, the SQUEEZE[S8] routine included in PLATON[S9] was applied and a density of 426 e^- in an approximately 1400 $Å^3$ volume was identified. This density fits reasonably well with the presence of 7 molecules of chlorobenzene and possibly one extra molecule of methanol in the unit cell, solvents used in the crystallization. This density was removed and the data refined against the model. These solvent molecules removed with SQUEEZE were added to the cell unit contents and a last cycle of refinement was performed. Additionally, SIMU, DELU and ISOR instructions were used to model the disorder associated with a molecule of chlorobenzene present in the crystal of **1** and that of one of the *t*-butyl groups in **6**. Both compounds have crystallized as a racemic mixture of the *P* and *M* enantiomers.

Table S3. Summary of X-ray diffraction crystallography measurement and refinement data for compounds **1** and **6**[a]

	1·5.5C_6H_5Cl·0.5CH_3OH	**6**·2C_6H_{14}
Chemical formula	$C_{140.5}H_{113.5}Cl_{5.5}O_{1.5}$	$C_{116}H_{103}F_3O_4S$
M_r	2020.78	1650.04
Crystal size [mm^3]	0.444 x 0.140 x 0.040	0.453 x 0.088 x 0.038
Crystal system	Triclinic	Triclinic
Space group	*P*-1	*P*-1
a [Å]	15.3025(6)	14.3675(8)
b [Å]	16.0955(6)	17.3718(11)
c [Å]	22.2445(9)	18.9206(12)
α [°]	94.998(2)	67.525(3)
β [°]	108.991(2)	86.143(3)
γ [°]	92.221(2)	89.598(3)
V [Å^3]	5147.8(4)	4352.9(5)
Z	2	2
ρ_{calcd} [Mg m^{-3}]	1.304	1.259
μ [mm^{-1}]	1.845	0.835
F(000)	2124	1748
θ range [°]	2.112 to 59.291	2.533 to 50.604
hkl ranges	-16,17/-17,17/-24,24	-14,14/-17,17/ -18,18
Reflections collected	64348	41843
Independent reflections	14785	9165
R_{int}	0.0391	0.0523
Completeness [%]	98.9%	99.7 %
Absorption correction	Numerical	Multi-scan
Final *R* indices [$I>2\sigma(I)$]	R_1 = 0.0996 wR_2 = 0.2829	R_1 = 0.0720 wR_2 = 0.1869
R indices (all data)	R_1 = 0.1171 wR_2 = 0.3003	R_1 = 0.0872 wR_2 = 0.2004
Goodness-of-fit on F^2	1.054	1.036

[a]In common: Temperature, 100 K. Wavelength, 1.54178 Å (Cu-Kα). Refinement method, full-matrix least-squares on F^2.

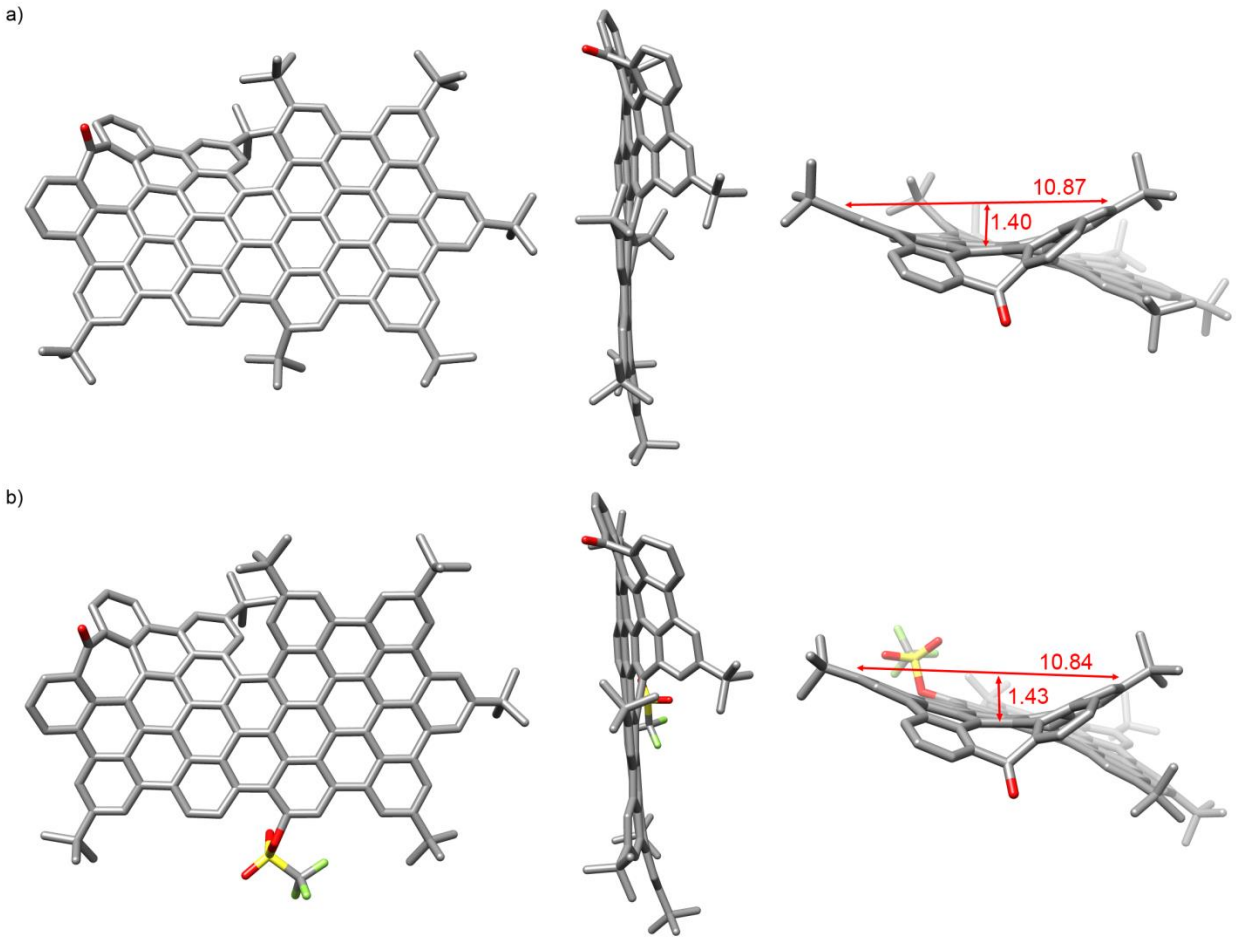

Figure S27. Top view (left), side view (middle) and front view showing the dimensions (in Å) of the aromatic saddle-shaped region (right) of the crystal structure of: a) **1**, b) **6**. Hydrogen atoms and solvent molecules have been omitted for clarity. The width of the aromatic saddles correspond to the C(sp^2)– C(sp^2) distance, while the depth has been calculated as the distance between the centroid of the width and the mean plane of the closest aromatic ring.

Table S4. Relevant distances and angles in the x-ray structure of **1** and **6**[a]

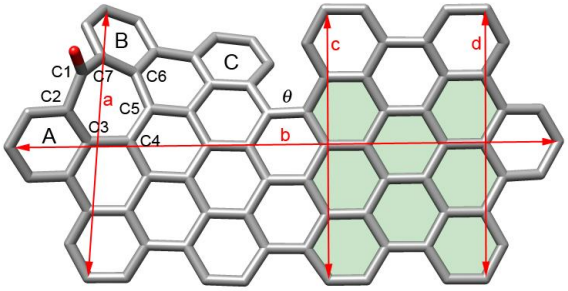

	1	**6**
Distance a [Å][a]	9.83	9.90
Distance b [Å][a]	19.83	19.78
Distance c [Å][a]	9.81	9.75
Distance d [Å][a]	9.82	9.77
Bond Distance C1–C2 [Å][b]	1.466(6)	1.471(6)
Bond Distance C2–C3 [Å][b]	1.422(6)	1.421(6)
Bond Distance C3–C4 [Å][b]	1.482(5)	1.482(6)
Bond Distance C4–C5 [Å][b]	1.432(5)	1.434(6)
Bond Distance C5–C6 [Å][b]	1.486(5)	1.477(6)
Bond Distance C6–C7 [Å][b]	1.407(5)	1.409(6)
Bond Distance C1–C7 [Å][b]	1.464(6)	1.469(6)
Angle θ [º][c]	29.8	33.2
Angle A-planar region [º][d]	24.1[e]	20.4
Angle B-planar region [º][d]	48.6[e]	48.6
Angle C-planar region [º][d]	40.1[e]	45.6

[a]C–C distance, measured with the CCDC Mercury software.[S10] [b]From the cif file. [c]Torsional angle (absolute value). [d]Angle between the mean plane of the labeled aromatic ring and the mean plane of the planar region (colored in green). [e]In this case one of the edge atoms of the planar region was not considered for calculating the mean plane due to a distortion induced by the presence of a *t*-butyl group.

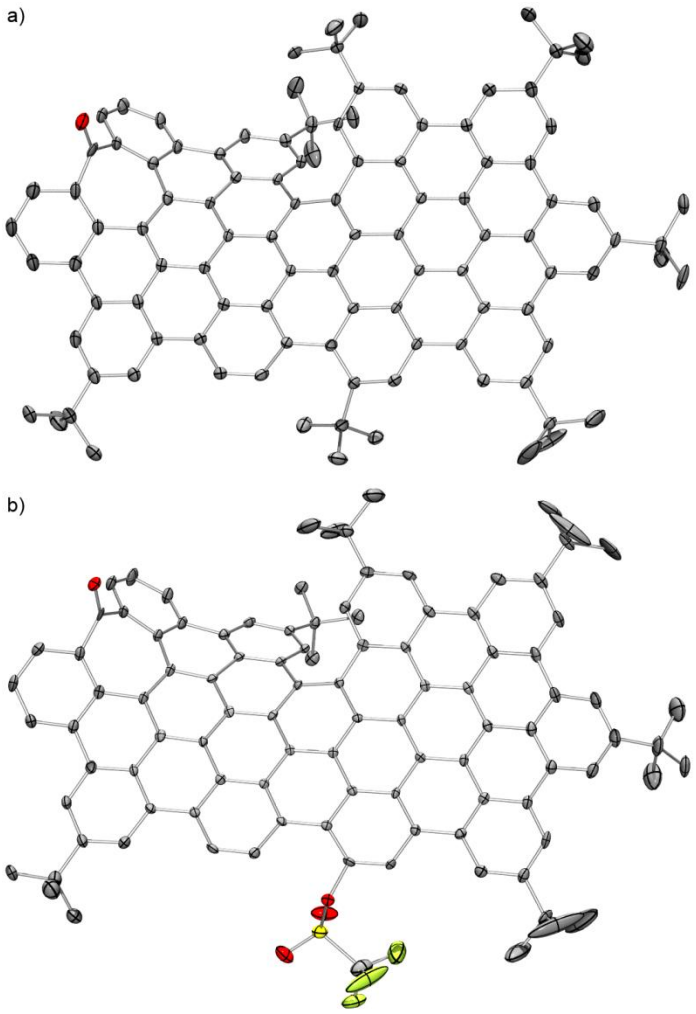

Figure S28. ORTEP drawing showing the thermal displacement ellipsoids (50% probability) of the crystal structure of: a) **1**; b) **6**. Hydrogen atoms and solvent molecules have been omitted for clarity**.**

Theoretical calculations

Calculations were done using Gaussian 09.[S11] Ground state geometry optimizations were performed in vacuum for the different molecules at the B3LYP/6-31G(d,p) level, and frequency calculations were used to ensure that a minimum was reached. TDDFT calculations were done at the same level of approximation to estimate the Franck − Condon transition energies and the corresponding configuration interaction coefficients, transition dipole moments, and oscillator and rotatory strengths for one-photon absorption.

The overall agreement between calculated absorption and CD spectra at the B3LYP/6-31G(d,p) level of theory and the corresponding experimentally observed spectra is very good. Noteworthy is the fact that the lowest energy transition in the CD spectrum of *M*-**1** is predicted with a positive sign when the observed sign is negative, and vice-versa for *P*-**1**. This transition has both a weak oscillator and rotatory strength whose relative magnitude in module is correctly predicted by the calculations. Being aware that calculation of bands with weak oscillatory and rotational strengths might be highly influenced by the functional and the basis set used, we also carried out DFT calculations of *M*-**1** at the CAM-B3LYP(6-31G(d,p) level of theory but, despite the fact that at this level of theory the sign of the lowest energy transition is correctly predicted by the calculations, the overall agreement between the experimental data and the calculated transitions was not improved. Thus, only the best results in reproducing the experimental CD are included in the main text, which were obtained with the B3LYP functional.

We have optimized both diastereoisomers of compound *M*-**1** with the saddle tropone 'up': *anti*-*M*-**1** and 'down': *syn*-*M*-**1** to the closer ^{t}Bu group of the *M*-helicene moiety. The DFT (B3LYP/6-31G(d,p)) theoretical free energy of the two diastereoisomers of *M*-1 showed that the *anti*-*M*-**1** diastereoisomer is the most stable one (ΔG=12 kcal/mol) which is in agreement with the diastereoisomers observed in the X-Ray structures of both compounds **1** and **6**.

Therefore, in the ground state the population of the higher energy diastereoisomer *syn*-*M*-**1** can be neglected at room temperature due to the relatively large energy difference that separates the two diastereoisomers.

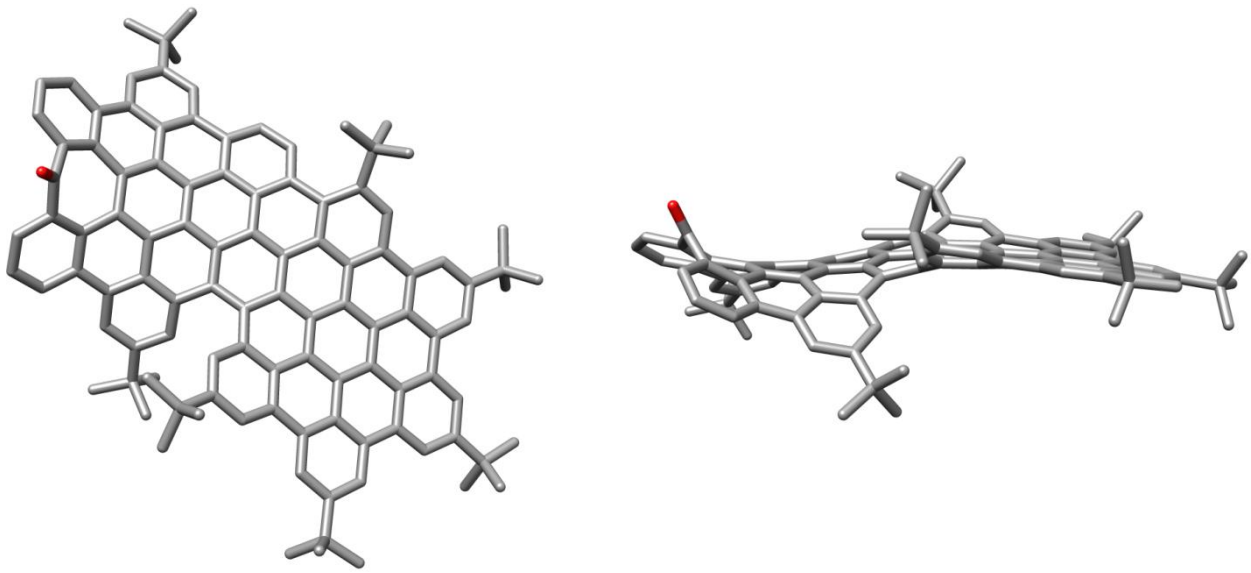

Figure S29. Top (left) and side (right) views of the DFT (B3LYP/6-31G(d,p)) calculated structure of *anti*-*M*-**1**, the diasteroisomer with the tropone moiety *anti* respect to the closer ^{t}Bu group of the *M*-helicene moiety. Hydrogen atoms have been omitted for clarity.

Table S5. Molecular orbitals involved in the lower energy electronic transitions (>300 nm) predicted by TDDFT at the B3LYP/6-31G(d,p) level for *M*-**1** in vacuum: orbitals involved (H, HOMO and L, LUMO), percentage contribution of each excitation to the CI expansion (%), wavelength of the transition (nm), oscillator strength (*f*) and rotatory strength in velocity form (R_{vel}, 10^{-40} cgs)

	Exp.	Calc.					
	λ^{exp}(nm)	λ^{calc} (nm)	H-n→L+m		CI	*F*	R_{vel} *M-1*
S_1	555	527	H-1	L	22	0.003	0.1
			H	L+1	19		
S_2	493	507	H	L	29	0.117	11.5
			H-1	L+1	12		
S_3	475	464	H-1	L+1	31	1.129	-83.4
			H	L	13		
S_4	444	449	H	L+1	19	0.426	57.5
			H-1	L	18		
S_5		446	H	L+2	16	0.017	11.3
			H-2	L	11		
S_6		430	H	L+3	12	0.042	-35.8
			H	L+2	11		
			H-2	L	10		
S_7		427	H-1	L+2	23	0.050	15.4
			H	L+2	17		
S_8		420	H-2	L	11	0.004	-34.4
			H-2	L+1	12		
S_9	397	409	H	L+3	15	0.147	66.2
			H-3	L	14		
S_{10}		407	H-1	L+3	29	0.173	-59.0
S_{11}		401	H-2	L+1	15	0.051	-46.7
S_{12}		397	H-3	L+1	31	0.080	-105.7
S_{13}	384	385	H	L+4	24	0.160	12.4
S_{14}	375	380	H-1	L+4	24	0.055	-12.6
S_{15}		380	H	L+6	28	0.002	-127.0
S_{16}		374	H-1	L+6	14	0.007	58.6
S_{17}		371	H-1	L+6	13	0.010	-46.1
S_{18}		367	H	L+6	20	0.022	24.0
			H-3	L+2	12		
S_{19}		365	H-2	L+2	32	0.079	5.7
.7S_{20}		361	H-1	L+5	10	0.043	-5.1
S_{21}		359	H-1	L+6	22	0.036	0.0
S_{22}		357	H-5	L	19	0.010	-35.8
S_{23}		356	H-5	L	13	0.066	-78.7
S_{24}	351	351	H-4	L+3	29	0.138	103.5
S_{25}		345	H	L+7	26	0.026	-57.1
S_{26}		343	H-3	L+3	15	0.015	-0.1
S_{27}		342	H-5	L+1	15	0.022	-26.3
			H-1	L+7	14		
S_{28}		339			-	0.018	13.1
S_{29}		337	H-1	L+7	12	0.008	9.7
S_{30}		334	H	L+9	29	0.005	-12.7
S_{31}		333	H-2	L+4	19	0.092	39.4
S_{32}		332	H-4	L+2	20	0.062	25.3
S_{33}		328	H-1	L+8	39	0.010	-23.0
S_{34}	312	327	H-2	L+5	17	0.128	-65.9
S_{35}		326	H-1	L+7	10	0.017	18.0
S_{36}		325	H-3	L+5	22	0.013	41.2
S_{37}		324	H-6	L+2	21	0.070	-41.2
S_{38}		324	H-6	L	28	0.031	-4.7
S_{39}		323	H-7	L+1	11	0.018	-5.6
S_{40}		321	H-1	L+9	20	0.007	34.0
S_{41}		320	H-4	L+3	20	0.108	29.5
S_{42}		318	H-8	L	10	0.028	9.3
			H-4	L+1	10		
S_{43}		317			-	0.047	-52.2
S_{44}		317	H-8	L	13	0.026	-33.9
S_{45}		316	H-6	L+1	14	0.058	7.5
S_{46}		315	H-1	L+9	11	0.062	4.1
S_{47}		315	H-9	L	14	0.042	32.4
S_{48}		314			-	0.007	11.1
S_{49}		313	H	L+10	11	0.036	9.5
S_{50}		312	H-9	L+1	12	0.032	-6.6

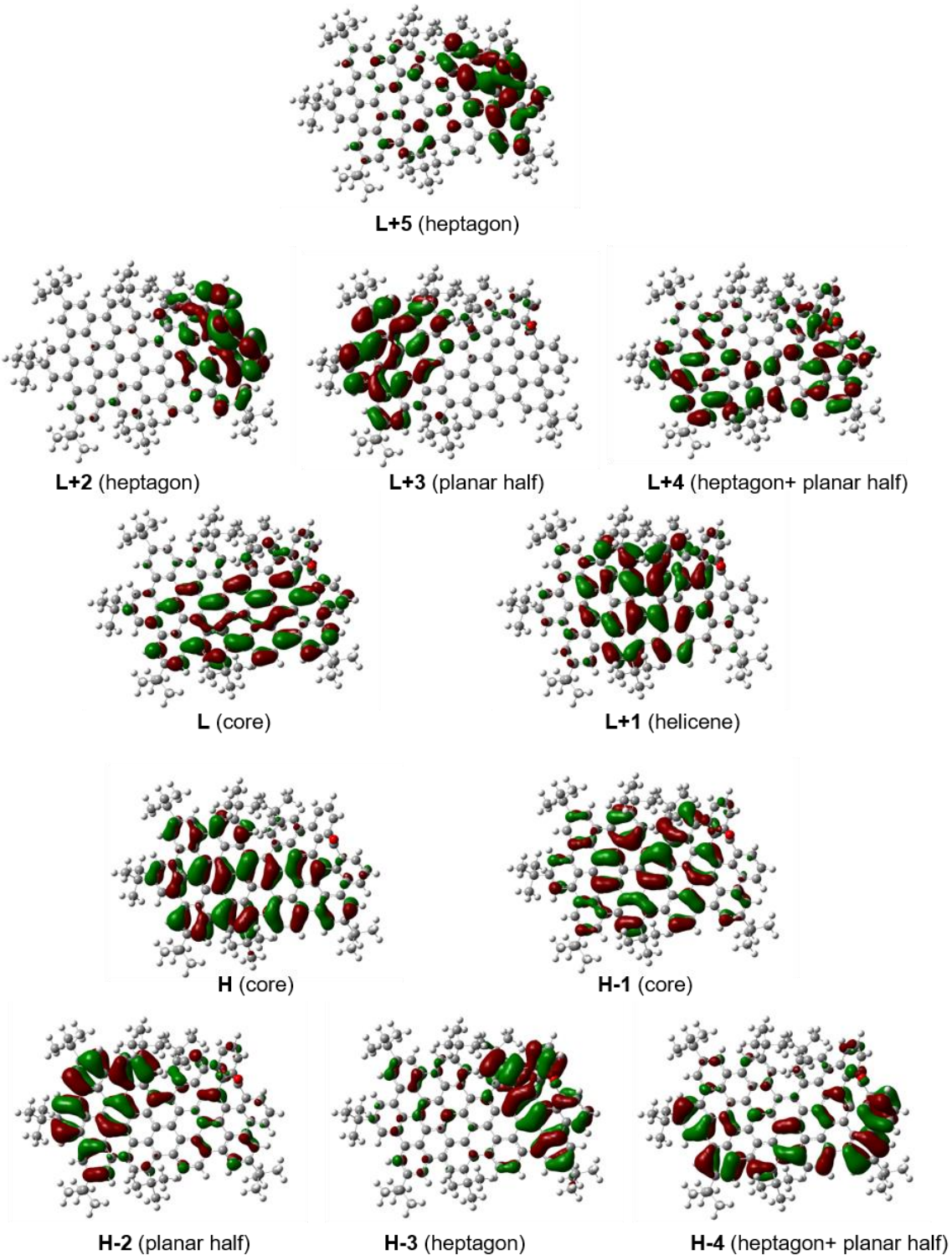

Figure S30. Isodensity surface for the frontier molecular orbitals of *anti-M*-**1** involved in lowest energy transitions observed. A brief description of the localization of the electron density is given in parenthesis: planar half, planar half of the molecules; core, sp^2 network including the helicene; heptagon, distorted half of the molecule including the heptagon; helicene, transitions localized in the helicene.

Table S6: Atomic coordinates for the DFT optimized structure of *anti-M*-**1**.

Atom	X	Y	Z
H	-9.110724	-1.240170	0.609415
C	3.626722	-0.359110	-0.112356
C	4.447010	0.783461	-0.123574
C	6.467264	-0.649056	-0.324568
C	5.632681	-1.816200	-0.212832
C	4.232996	-1.636949	-0.000651
C	5.861328	0.633946	-0.114035
C	3.397489	-2.697685	0.505354
C	6.652464	1.797563	0.210467
C	6.098657	-3.217690	-0.181091
C	2.189985	-0.224919	-0.142106
C	7.922346	-0.640198	-0.580910
C	3.842032	2.092316	-0.091701
C	8.697770	0.496532	-0.190049
C	5.339370	-4.189595	0.544460
C	1.360786	-1.354227	0.037347
C	4.623367	3.229278	0.201336
C	1.996084	-2.519488	0.655462
C	8.052022	1.681337	0.366261
C	3.997509	-3.867678	1.022783
C	6.040130	3.054355	0.487055
C	8.607011	-1.635045	-1.330134
C	9.968353	-1.531869	-1.629030
C	10.079265	0.538971	-0.457309
C	10.721261	-0.463493	-1.160399
C	2.439199	2.225688	-0.323541
C	1.848733	3.511998	-0.429252
C	3.981002	4.483319	0.250827
C	2.646335	4.617256	-0.063778
C	7.207517	-3.706468	-0.910644
C	7.614350	-5.041285	-0.837124
C	5.814955	-5.508150	0.659102
C	6.954517	-5.934558	-0.002476
C	1.611399	1.058091	-0.344325
C	0.205961	1.204311	-0.365710
C	-0.033750	-1.249027	-0.249326
C	-0.618690	0.041877	-0.317010
C	1.297602	-3.381784	1.513455
C	3.263170	-4.693984	1.883720
C	1.922174	-4.437048	2.187479
C	6.815161	4.085065	1.032985
C	8.776540	2.729092	0.953922
C	8.176128	3.935889	1.315760
C	8.002939	-2.884850	-1.855267
O	8.329919	-3.334877	-2.946380
C	8.949469	5.084867	1.989336
C	10.430851	4.736337	2.226658
C	8.305646	5.401810	3.360364
C	8.888734	6.343645	1.091692
C	1.131891	-5.260124	3.223121
C	2.004504	-6.324980	3.914356
C	0.581581	-4.310881	4.314740
C	-0.047765	-5.978969	2.529349
H	10.414680	-2.309707	-2.237489
H	10.647323	1.412686	-0.164300
H	11.782611	-0.393912	-1.377166
H	4.538934	5.371630	0.522285
H	2.185040	5.591905	0.010566
H	8.449746	-5.357980	-1.451105
H	5.237105	-6.231421	1.221739
H	7.287972	-6.964104	0.082615
H	0.246887	-3.186380	1.687049
H	3.760298	-5.532416	2.351742
H	6.332433	5.021423	1.283860
H	9.830531	2.588576	1.147071
H	10.934022	5.579096	2.711066
H	10.545056	3.865122	2.879934
H	10.958583	4.534007	1.288814
H	8.340094	4.529431	4.020848
H	8.841218	6.221844	3.851700
H	7.258485	5.701772	3.260441
H	9.428505	7.172719	1.562717
H	7.860069	6.673352	0.919289
H	9.345398	6.151536	0.115408
H	1.405738	-6.868282	4.652201
H	2.852446	-5.876916	4.442715
H	2.393180	-7.061540	3.203318
H	1.395766	-3.785098	4.823836
H	0.022502	-4.880585	5.065240
H	-0.093528	-3.557909	3.898889
H	-0.642166	-6.532971	3.264552
H	-0.713835	-5.277642	2.019419
H	0.318530	-6.693541	1.784898
C	-2.633719	1.473858	-0.271749
C	-0.386244	2.508544	-0.511539
C	-1.802084	2.633464	-0.425296
C	-2.052372	0.183078	-0.298007
C	-2.886417	-0.961355	-0.277981
C	-0.889148	-2.398222	-0.558799

C	-2.300318	-2.257140	-0.477312
C	-0.360824	-3.604197	-1.056896
C	-1.169140	-4.687889	-1.396571
C	-3.131929	-3.391258	-0.693768
C	-2.547098	-4.571443	-1.161126
C	0.434780	3.651930	-0.747124
C	-0.202915	4.855377	-1.215583
C	-2.380507	3.916010	-0.504164
C	-1.566734	4.965202	-0.970501
C	-4.038309	1.621428	-0.131458
C	-4.617945	2.935722	-0.059018
C	-3.800534	4.087668	-0.225170
C	-4.293735	-0.818559	-0.172707
C	-4.574232	-3.271599	-0.448044
C	-5.136685	-1.987505	-0.196149
C	-6.013503	3.097961	0.174378
C	-6.532057	4.395158	0.256456
C	-4.376308	5.363036	-0.106193
C	-5.737300	5.542430	0.133954
C	-4.866625	0.471395	-0.050301
C	-6.285694	0.615880	0.154860
C	-6.861678	1.906755	0.311604
C	-5.413017	-4.389908	-0.443238
C	-6.794079	-4.295010	-0.236110
C	-6.536583	-1.866574	0.009673
C	-7.329792	-3.025390	-0.024051
C	-7.118597	-0.537718	0.236224
C	-8.478476	-0.366498	0.518707
C	-8.233804	2.008872	0.587949
C	-9.059898	0.891472	0.705345
C	-7.655593	-5.572182	-0.251308
C	-10.563158	0.995721	1.026979
C	-6.383641	6.934991	0.265320
C	0.415371	5.965005	-2.133196
C	-0.611942	-5.961017	-2.063099
H	-4.977016	-5.370525	-0.590101
H	-8.396868	-2.931190	0.113929
H	-3.186837	-5.409994	-1.406163
H	0.706224	-3.667260	-1.209780
H	-8.666683	2.988705	0.726433
H	-2.059623	5.888339	-1.243499
H	-3.732574	6.228554	-0.182451
H	-7.593380	4.527199	0.422867
C	-0.583750	6.237687	-3.297711
H	-0.819765	5.315853	-3.837461
H	-1.523559	6.683730	-2.965828
H	-0.130498	6.939157	-4.005574
C	1.725397	5.550745	-2.843550
H	1.950938	6.286784	-3.621981
H	2.591266	5.500451	-2.187770
H	1.616807	4.576286	-3.329846
C	0.611219	7.301097	-1.378370
H	1.362603	7.236635	-0.587015
H	0.936564	8.081869	-2.075112
H	-0.324032	7.633579	-0.916640
C	-7.453480	7.111019	-0.838765
H	-8.239232	6.353227	-0.770206
H	-7.930730	8.093716	-0.753402
H	-7.004610	7.036163	-1.834497
C	-5.356617	8.074091	0.122957
H	-4.583352	8.024159	0.896432
H	-4.865444	8.060561	-0.855553
H	-5.861723	9.039906	0.223731
C	-7.053625	7.065086	1.653962
H	-7.519166	8.051273	1.761069
H	-7.833247	6.312701	1.804430
H	-6.317842	6.947554	2.456025
C	-11.028083	2.453757	1.202946
H	-10.507206	2.951850	2.027252
H	-10.875342	3.043274	0.292960
H	-12.098526	2.473447	1.430787
C	-10.861514	0.235468	2.341324
H	-10.595435	-0.823203	2.270893
H	-10.300495	0.664562	3.177822
H	-11.928969	0.294513	2.581369
C	-11.381391	0.367598	-0.126298
H	-11.194864	0.891629	-1.069289
H	-11.132268	-0.686869	-0.276828
H	-12.453846	0.428186	0.090288
C	-9.149844	-5.278769	-0.018313
H	-9.327004	-4.808209	0.954359
H	-9.564467	-4.628848	-0.795902
H	-9.714943	-6.216017	-0.038073
C	-7.174798	-6.528651	0.865930
H	-6.128103	-6.817816	0.734032
H	-7.268976	-6.059115	1.850464
H	-7.775308	-7.445263	0.867152
C	-7.513755	-6.272924	-1.623376
H	-6.477042	-6.550540	-1.834511
H	-8.114850	-7.188786	-1.648097
H	-7.855164	-5.620001	-2.433159
C	-1.141388	-6.028369	-3.516413
H	-0.764354	-6.926010	-4.019643
H	-2.234863	-6.060247	-3.546722
H	-0.817175	-5.154937	-4.091139
C	0.928130	-5.972171	-2.108051

H	1.325991	-5.150697	-2.712022
H	1.366870	-5.902511	-1.107529
H	1.275286	-6.906145	-2.561385
C	-1.077617	-7.220506	-1.296374
H	-2.167288	-7.313525	-1.273521
H	-0.682871	-8.121308	-1.778837
H	-0.722016	-7.206429	-0.261769

(0 imaginary frecuencies)
Zero-point correction = 1.589247 (Hartree/Particle)
Thermal correction to Energy = 1.676331
Thermal correction to Enthalpy = 1.677275
Thermal correction to Gibbs Free Energy = 1.470418
Sum of electronic and zero-point Energies = –4202.164207
Sum of electronic and thermal Energies = –4202.077123
Sum of electronic and thermal Enthalpies = –4202.076179
Sum of electronic and thermal Free Energies = –4202.283036

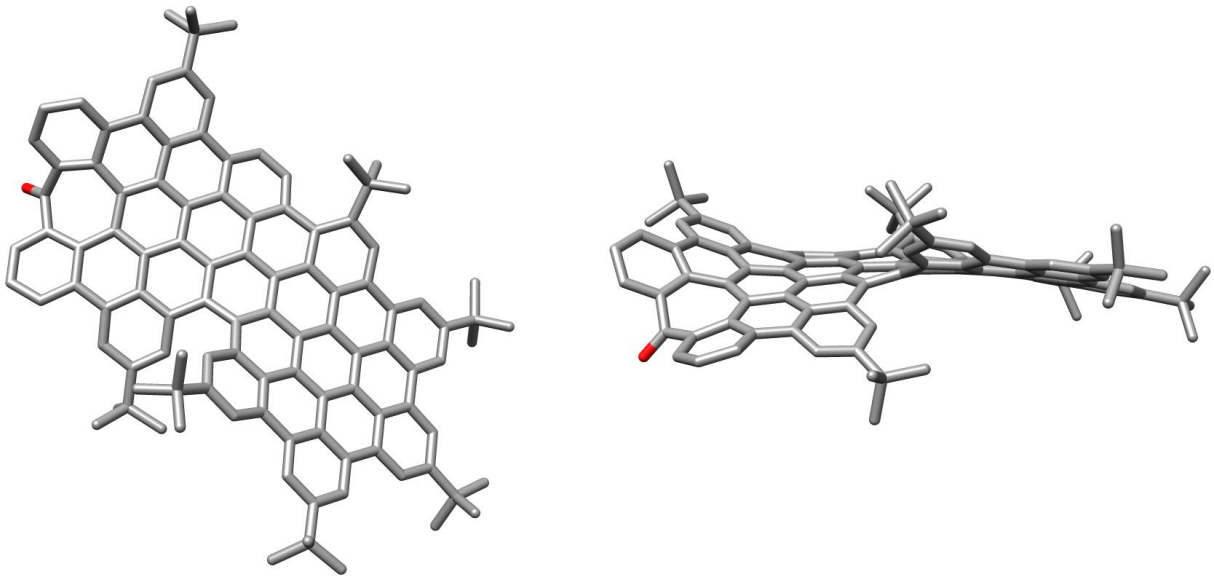

Figure S31. Top (left) and side (right) views of the DFT (B3LYP/6-31G(d,p)) calculated structure of *syn*-*M*-**1**, the diasteroisomer with the tropone moiety *syn* respect to the closer ^{t}Bu group of the *M*-helicene moiety. Hydrogen atoms have been omitted for clarity.

Table S7: Atomic coordinates for the DFT optimized structure of *syn*-*M*-**1**.

Atom	X	Y	Z
C	6.767417	-4.104533	1.279884
C	5.377599	-4.174669	1.430115
C	4.534900	-3.092652	1.156835
C	5.110376	-1.878774	0.679191
C	6.518979	-1.782284	0.524473
C	7.311333	-2.898909	0.836526
C	4.270443	-0.748201	0.380236
C	2.861664	-0.882752	0.445406
C	2.027935	0.235479	0.211096
C	2.603024	1.501765	-0.034991
C	4.010735	1.632232	-0.153055
C	4.844142	0.498019	0.026568
C	5.691387	5.433763	-1.161227
C	6.497172	4.294498	-1.031279
C	5.986629	3.036609	-0.690572
C	4.586072	2.911105	-0.465810
C	3.757139	4.063885	-0.548477
C	4.326974	5.294757	-0.910824
C	2.265656	-2.120357	0.859306
C	1.761347	2.660918	-0.108430
C	6.269178	0.614949	-0.144043
C	3.079689	-3.182520	1.333362
C	2.462453	-4.264971	1.977038
C	1.075035	-4.343132	2.145559
C	0.289389	-3.347986	1.554928
C	0.849071	-2.255944	0.875717
C	6.845228	1.853001	-0.543265
C	8.228226	1.913152	-0.773201
C	9.063098	0.807221	-0.614646
C	8.479228	-0.392274	-0.193765
C	7.108062	-0.520244	0.055206
C	0.343957	2.547945	-0.002088
C	-0.481301	3.709462	0.101251
C	0.172153	4.972303	0.371894
C	1.522110	5.045745	0.050688
C	2.335123	3.937396	-0.251443
C	-6.068712	-3.196791	-1.333224
C	-7.365473	-3.515250	-1.836122
C	-8.512149	-2.594146	-1.935422

C	-8.834715	-1.785111	-0.746578
C	-7.940853	-0.824164	-0.218762
C	-6.478428	-0.754163	-0.463662
C	-5.618103	-1.869231	-0.831070
C	-10.140957	-1.946697	-0.279508
C	-10.611139	-1.164702	0.768196
C	-9.839998	-0.083952	1.160151
C	-8.575912	0.166930	0.596541
C	-5.130314	-4.273144	-1.446876
C	-5.561768	-5.586559	-1.721393
C	-6.853995	-5.868630	-2.111806
C	-7.729676	-4.802091	-2.246961
C	-5.871596	0.512732	-0.170360
C	-4.462134	0.698723	-0.221052
C	-3.622004	-0.426472	-0.349842
C	-4.193700	-1.701976	-0.645830
O	-9.295884	-2.641888	-2.875487
C	-6.662523	1.659730	0.227880
C	-3.254750	-2.782268	-0.868265
C	-7.984015	1.491266	0.694358
C	-8.729678	2.603704	1.103112
C	-8.217375	3.905296	1.070949
C	-6.910920	4.062028	0.614815
C	-6.125049	2.972456	0.203864
C	-1.851355	-2.610522	-0.691751
C	-0.966159	-3.575854	-1.207447
C	-1.401634	-4.750525	-1.810291
C	-2.780029	-4.974570	-1.827085
C	-3.701279	-4.034076	-1.348320
C	-3.889633	2.022847	-0.137874
C	-2.194488	-0.252545	-0.167673
C	-4.729301	3.154575	-0.133556
C	-4.152403	4.413174	-0.395075
C	-2.785114	4.574952	-0.405344
C	-1.910011	3.512207	-0.092087
C	-2.476808	2.205203	-0.089468
C	-1.637477	1.055453	-0.034152
C	-0.236718	1.230727	0.015647
C	0.597324	0.087369	0.180337
C	0.021855	-1.197979	0.288840
C	-1.334641	-1.370074	-0.134113
C	-9.094412	5.087137	1.523623
C	-8.350831	6.433815	1.442086
C	-9.536590	4.869367	2.989914
C	-10.345138	5.172274	0.616853
C	-0.445499	-5.740966	-2.500953
C	-0.670640	-5.656857	-4.030288
C	-0.729882	-7.185365	-2.028035
C	1.033686	-5.424654	-2.207887
C	-0.393092	6.204558	1.166232
C	0.709572	6.713401	2.145100
C	-1.579866	5.853795	2.095136
C	-0.739560	7.397830	0.243436
C	0.401476	-5.455000	2.974423
C	1.418505	-6.456807	3.552907
C	-0.596388	-6.240348	2.092699
C	-0.360341	-4.807972	4.156398
H	-0.789046	-3.398289	1.641152
H	9.119194	-1.256169	-0.068378
H	2.019278	5.999612	0.156283
H	-10.767402	-2.696086	-0.749942
H	-11.586937	-1.342315	1.208930
H	-10.232983	0.608168	1.895536
H	-4.850774	-6.397873	-1.633574
H	-7.163791	-6.884547	-2.335144
H	-8.731475	-4.942055	-2.634291
H	-9.756520	2.458855	1.413380
H	-6.461187	5.045273	0.612988
H	0.090079	-3.362068	-1.166282
H	-3.150084	-5.870961	-2.304667
H	-4.788861	5.268374	-0.594414
H	-2.369664	5.541485	-0.646509
H	-8.038626	6.666121	0.418674
H	-7.463897	6.451142	2.084000
H	-9.013258	7.239565	1.774015
H	-10.113364	3.947557	3.109153
H	-8.669777	4.808726	3.655985
H	-10.166174	5.700885	3.325633
H	-10.944607	4.258462	0.661528
H	-10.060701	5.333295	-0.427934
H	-10.984649	6.005943	0.927904
H	-0.461743	-4.648213	-4.400813
H	-1.701929	-5.904376	-4.300007
H	-0.008219	-6.355810	-4.553598
H	-1.746668	-7.508823	-2.269563
H	-0.041982	-7.882872	-2.518122
H	-0.596293	-7.281592	-0.946286
H	1.329726	-4.447628	-2.601974
H	1.671335	-6.174172	-2.687539
H	1.249462	-5.438246	-1.134795
H	1.565662	7.163790	1.638085
H	1.079060	5.904579	2.782097
H	0.283418	7.487259	2.791331
H	-2.507706	5.632151	1.575534
H	-1.335631	4.992073	2.724564
H	-1.773777	6.703528	2.757962

H	-1.565690	7.194399	-0.441397
H	0.125554	7.681835	-0.364555
H	-1.024244	8.267036	0.847045
H	1.977313	-6.972615	2.764741
H	0.892189	-7.219983	4.134775
H	2.136206	-5.970633	4.221680
H	-1.356259	-5.590694	1.650195
H	-0.074760	-6.748273	1.275082
H	-1.112040	-7.002008	2.688226
H	-1.132862	-4.114427	3.812425
H	0.323874	-4.250660	4.804468
H	-0.849913	-5.579118	4.761632
H	8.663256	2.849086	-1.091393
H	7.560078	4.400770	-1.206377
H	3.675903	6.151266	-1.020533
H	8.383944	-2.822084	0.735742
H	4.938824	-5.109915	1.755240
H	3.084345	-5.039302	2.403704
C	10.580124	0.863686	-0.879794
C	10.947555	-0.152174	-1.987519
H	12.025017	-0.126308	-2.185702
H	10.686675	-1.176528	-1.706119
H	10.424663	0.080185	-2.920875
C	11.046727	2.258357	-1.338271
H	10.563888	2.563032	-2.272482
H	10.848118	3.024828	-0.581955
H	12.126730	2.244222	-1.515740
C	11.342794	0.505915	0.418251
H	11.104432	1.212952	1.219450
H	11.093451	-0.497603	0.774781
H	12.424474	0.538429	0.246000
C	6.331388	6.775008	-1.568525
C	5.299654	7.915222	-1.659999
H	4.528276	7.709855	-2.409370
H	4.806036	8.096713	-0.699629
H	5.802326	8.842806	-1.951827
C	7.005228	6.624589	-2.953150
H	7.783753	5.856265	-2.946015
H	6.271845	6.348480	-3.717667
H	7.471895	7.569035	-3.254706
C	7.396572	7.176659	-0.520487
H	8.192363	6.430582	-0.438120
H	7.862116	8.129220	-0.797294
H	6.945968	7.293895	0.470393
C	7.631901	-5.339228	1.600357
C	7.217920	-6.508432	0.675159
H	6.166360	-6.780001	0.805662
H	7.366072	-6.245709	-0.377272
H	7.820374	-7.397757	0.891890
C	9.135449	-5.075504	1.393151
H	9.364105	-4.808458	0.356152
H	9.502866	-4.274749	2.043411
H	9.703872	-5.979841	1.632306
C	7.416766	-5.751919	3.076003
H	8.024284	-6.631124	3.318121
H	7.704174	-4.942489	3.754811
H	6.372380	-6.003863	3.281887

(0 imaginary frecuencies)
Zero-point correction = 1.589305 (Hartree/Particle)
Thermal correction to Energy = 1.676361
Thermal correction to Enthalpy = 1.677305
Thermal correction to Gibbs Free Energy = 1.469895
Sum of electronic and zero-point Energies = –4202.144747
Sum of electronic and thermal Energies = –4202.057691
Sum of electronic and thermal Enthalpies = –4202.056747
Sum of electronic and thermal Free Energies = –4202.264157

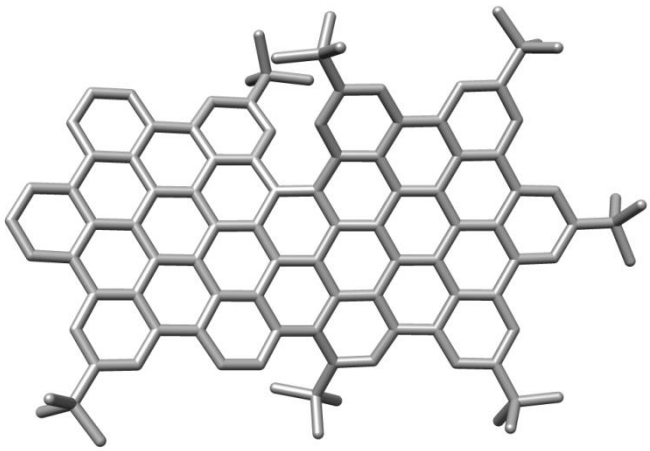

Figure S312. DFT (B3LYP/6-31G(d,p)) calculated structure of a purely hexagonal analogue of **1**. Hydrogen atoms have been omitted for clarity.

Table S8. Atomic coordinates for the DFT optimized structure of purely hexagonal analogue of **1**.

Atom	X	Y	Z
C	-8.548464	-2.276691	0.087682
C	-7.966894	-0.997554	-0.155761
C	-6.547135	-0.806283	0.021076
C	-5.728199	-1.893079	0.422826
C	-6.313142	-3.171753	0.748756
C	-7.714352	-3.370839	0.591848
C	-9.918530	-2.453630	-0.155893
H	-10.381236	-3.420472	-0.003320
C	-10.706610	-1.405121	-0.609518
H	-11.763663	-1.565678	-0.799353
C	-10.149153	-0.150833	-0.820627
H	-10.791842	0.645751	-1.173634
C	-8.785154	0.084186	-0.596919
C	-8.262196	-4.615998	0.937163
H	-9.326790	-4.791123	0.846255
C	-7.459584	-5.645613	1.408743
H	-7.903053	-6.604579	1.659675
C	-6.091562	-5.455527	1.560569
H	-5.487598	-6.283338	1.911661
C	-5.493505	-4.226795	1.250356
C	-4.051176	-4.013773	1.411657
C	-3.475893	-2.803931	0.933565
C	-4.321999	-1.722292	0.509641
C	-3.742450	-0.453493	0.271827
C	-4.567728	0.654992	-0.047920
C	-5.965826	0.471918	-0.210507
C	-6.789782	1.585149	-0.603526
C	-8.188796	1.409011	-0.802463
C	-8.961036	2.511771	-1.180837
H	-10.026291	2.384474	-1.321730
C	-8.418781	3.787557	-1.376019
C	-7.049747	3.942746	-1.175488
H	-6.611485	4.920779	-1.308829
C	-6.218385	2.875363	-0.794946
C	-3.987063	1.963791	-0.200856
C	-4.789912	3.066938	-0.571926
C	-4.150918	4.316912	-0.731647
H	-4.702866	5.168471	-1.110473
C	-2.824191	4.497969	-0.405442
H	-2.375452	5.470808	-0.551693
C	-2.020960	3.439730	0.070675
C	-2.590419	2.142715	0.038840
C	-1.747513	0.997883	0.183516
C	-2.310310	-0.299550	0.295054
C	-1.467066	-1.430846	0.395967
C	-2.062202	-2.649524	0.947230
C	-1.283535	-3.615481	1.611042
H	-0.221037	-3.439915	1.692675
C	-1.841332	-4.757331	2.182618
C	-3.221964	-4.952836	2.032501
H	-3.664386	-5.845700	2.455639
C	-0.089749	-1.282150	0.028282
C	0.484548	0.015906	0.050728
C	-0.346614	1.165535	0.189498
C	0.222614	2.480725	0.301989
C	-0.627868	3.618460	0.461885
C	-0.039635	4.838463	0.947293
C	1.342246	4.944065	0.837378
H	1.803446	5.870583	1.147569
C	2.199927	3.901227	0.444612
C	1.639897	2.618238	0.285292
C	2.486063	1.471304	0.089368
C	1.912774	0.182551	-0.049302
C	2.749911	-0.940953	-0.264868
C	2.152237	-2.219414	-0.532129
C	2.962983	-3.313532	-0.947162
C	2.341106	-4.457783	-1.454003
H	2.957006	-5.259983	-1.840628
C	0.947459	-4.576132	-1.551784
C	0.172743	-3.539929	-1.034629
H	-0.903613	-3.604741	-1.083827
C	0.740668	-2.378491	-0.476460
C	4.421358	-3.192131	-0.858234
C	4.999992	-1.927696	-0.567293
C	4.158857	-0.782499	-0.320889
C	4.734807	0.499730	-0.139923
C	3.897233	1.631191	0.050517
C	4.477282	2.943589	0.168882
C	3.640836	4.087735	0.314320
C	4.223088	5.361008	0.321094
H	3.577367	6.228891	0.375589
C	5.603630	5.556072	0.223486
C	6.411050	4.421071	0.134525
H	7.479937	4.552232	0.051944
C	5.886499	3.119000	0.112714
C	6.753075	1.939718	0.022596
C	6.168530	0.654506	-0.143193

C	7.014965	-0.482675	-0.287086
C	6.417070	-1.801339	-0.532236
C	7.200348	-2.940514	-0.752803
H	8.278728	-2.849324	-0.736837
C	6.649551	-4.202962	-0.996323
C	5.259386	-4.301234	-1.046228
H	4.807689	-5.268182	-1.215644
C	8.400294	-0.305927	-0.206789
H	9.046773	-1.169184	-0.296127
C	8.994139	0.943855	-0.002854
C	8.150703	2.048568	0.101035
H	8.588329	3.021928	0.267434
C	-9.340602	4.952160	-1.785726
C	-10.039909	4.611293	-3.123250
H	-10.646581	3.704095	-3.048621
H	-10.702958	5.429857	-3.424791
H	-9.306285	4.456416	-3.920961
C	-10.409833	5.170338	-0.688785
H	-9.942092	5.420405	0.268903
H	-11.078038	5.993158	-0.966641
H	-11.025654	4.279310	-0.536072
C	-8.571342	6.273649	-1.973106
H	-7.810641	6.196022	-2.756896
H	-9.267939	7.064973	-2.267840
H	-8.081033	6.595871	-1.048637
C	-0.746025	5.985101	1.749444
C	-2.095254	5.575910	2.385753
H	-2.905605	5.456266	1.671097
H	-1.997554	4.638179	2.941788
H	-2.400332	6.351952	3.095293
C	-0.916836	7.264127	0.895857
H	-1.318304	8.077137	1.511428
H	0.043993	7.595290	0.488603
H	-1.599118	7.125401	0.053623
C	0.152492	6.364806	2.964360
H	0.386734	5.486319	3.572840
H	1.094130	6.837889	2.677554
H	-0.381367	7.082328	3.595432
C	-1.008335	-5.775696	2.984734
C	-1.194689	-7.193410	2.395342
H	-2.237701	-7.521407	2.428038
H	-0.866244	-7.231965	1.351854
H	-0.603983	-7.920149	2.963818
C	0.495796	-5.443972	2.965854
H	0.896367	-5.425094	1.947282
H	0.706495	-4.476239	3.432063
H	1.047467	-6.204473	3.527728
C	-1.488766	-5.771069	4.456041
H	-0.911748	-6.490604	5.047993
H	-1.362043	-4.781254	4.906077
H	-2.545895	-6.041391	4.538840
C	0.334521	-5.804097	-2.252328
C	0.742028	-5.781989	-3.745485
H	0.322316	-6.648132	-4.269751
H	0.373862	-4.875881	-4.237186
H	1.828954	-5.809729	-3.868635
C	0.863001	-7.104462	-1.602774
H	1.950059	-7.195393	-1.685025
H	0.604783	-7.147634	-0.539886
H	0.422449	-7.978631	-2.094711
C	-1.203729	-5.819507	-2.170479
H	-1.588261	-6.719276	-2.661469
H	-1.558001	-5.827169	-1.134829
H	-1.648405	-4.956730	-2.676215
C	6.173244	6.987566	0.209944
C	7.710549	7.009947	0.110149
H	8.062905	8.046321	0.110273
H	8.182243	6.501897	0.957680
H	8.067137	6.541739	-0.813117
C	5.767726	7.716465	1.513142
H	4.681376	7.778946	1.624993
H	6.163948	7.197774	2.392084
H	6.161092	8.739170	1.515403
C	5.602313	7.756044	-1.005610
H	5.996721	8.778226	-1.029600
H	5.876803	7.263478	-1.943950
H	4.510946	7.821749	-0.971285
C	10.528075	1.052170	0.094451
C	11.163118	0.544247	-1.221907
H	10.899321	-0.497404	-1.427368
H	10.830813	1.145803	-2.074142
H	12.255781	0.605838	-1.166998
C	11.002259	2.499208	0.326512
H	12.094973	2.523249	0.387045
H	10.703930	3.162474	-0.492038
H	10.612244	2.911773	1.262813
C	11.031645	0.187722	1.274842
H	10.765988	-0.866368	1.152737
H	12.122885	0.248423	1.353559
H	10.602897	0.531237	2.221806
C	7.578538	-5.414660	-1.203276
C	8.479871	-5.165428	-2.435919
H	9.153790	-6.015010	-2.593793
H	7.877729	-5.036425	-3.341141
H	9.096315	-4.269728	-2.316214
C	6.796743	-6.720970	-1.439084

H	6.156080	-6.972264	-0.587486
H	6.170951	-6.665842	-2.335822
H	7.498510	-7.549372	-1.578802
C	8.464738	-5.606673	0.050372
H	7.851531	-5.786746	0.939284
H	9.132145	-6.465607	-0.082336
H	9.087897	-4.729730	0.248595

(0 imaginary frecuencies)

STM characterization

In order to test the feasibility of exploiting the ultimate resolution afforded by Surface Science techniques such as scanning tunneling microscopy (STM) under ultra-high vacuum (UHV) conditions, we have performed some preliminary tests on the deposition of **1** on a Cu(111) single crystal surface. The idea behind this study is trying to relate the macroscopic electronic and optoelectronic properties exhibited by this nanographene molecule to its topographical structure at the atomic level. However, the deposition of such big organic molecules on surfaces under HV/UHV conditions remains a big challenge as their large dimensions and molecular weight makes difficult their thermal sublimation before partial or total decomposition. To circumvent this problem, we have used a novel deposition method based on the injection inside the UHV system of microdroplets of a solution containing the molecule of interest by means of a fast pulsed valve.[S12] This system allows for the deposition of soluble molecules and macro-molecules without decomposition and a minimum solvent contamination. Figure S31 shows four room temperature (RT) STM images of the clean Cu(111) single crystal surface before (a) and after deposition of the CH_2Cl_2 solvent (control experiment, (b)) and of submonolayer coverage of **1** (c,d). As it can be clearly observed, the Cu surface is covered by homogeneously distributed elongated features with dimensions of approximately 2.3 nm and 1.3 nm along both axes, and 1.8 Å in apparent height, in contrast with the spikes associated to molecular diffusion observed when depositing the solvent. The good agreement between the dimensions obtained from STM and those extracted from X-ray crystallography allows us to assign these features to the nanographene molecule **1**, as can be observed in the scaled superimposed model in Figure S31c. Higher resolution STM images revealing the distorted geometry of **1** were impossible to obtain given the diffusion of both solvent and **1** at RT when trying to approach the tip, as evidenced by the appearance of horizontal spikes in the STM images. It is worthy to note the weak surface-molecule interaction, dominated by van der Waals forces between the π electrons of **1** and the electron gas of Cu(111) This interaction is weakened by the presence of the tert-butyl groups which further separate the molecular plane from the surface. Although LT-STM images are required to obtain high-resolution images of **1**, this preliminary study shows the feasibility of depositing **1** under ultra-clean conditions on a single crystal surface, opening a door towards in-depth atomic characterization of its electronic, optoelectronic, and chiral properties.

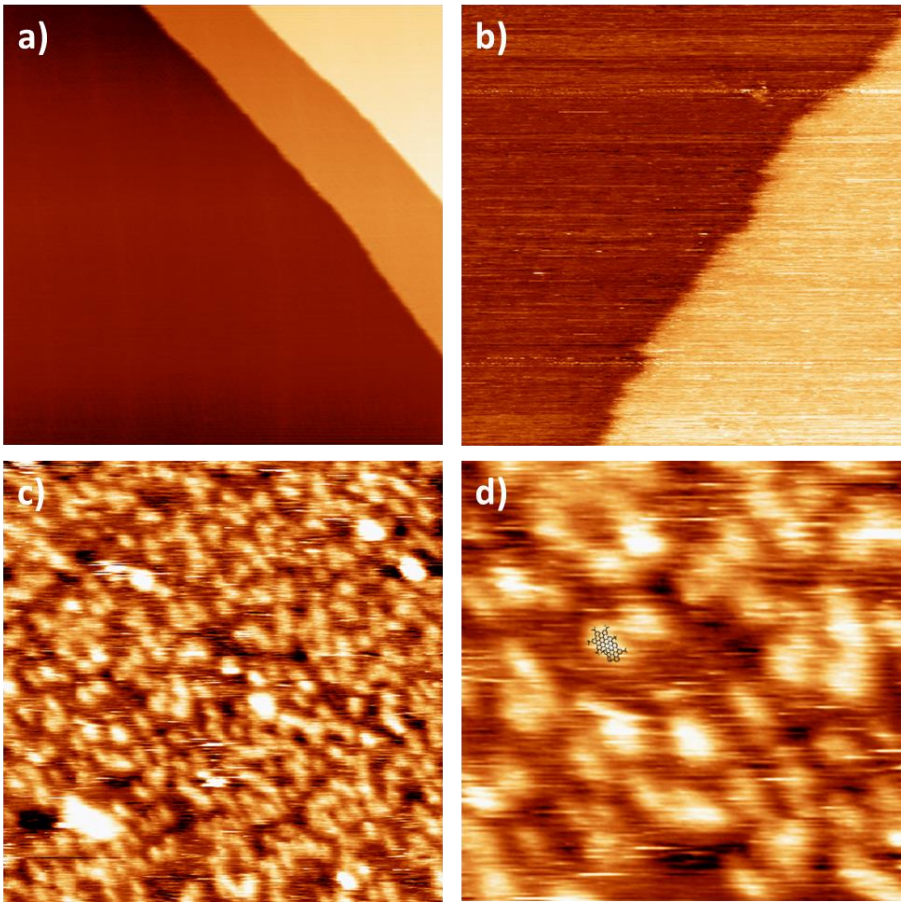

Figure 323. STM images of the clean Cu(111) surface (**a**), after CH_2Cl_2 deposition (**b**), and after deposition of submonolayer coverage of **1** under HV conditions (**c,d**). (a) Size: 100 nm x 100nm, I = 16 pA, V = 1.6 V; (b) Size: 50 nm x 50 nm, I = 25 pA, V = -1.0 V; (c) Size: 50 nm x 50 nm, I = 25 pA, V = 1.0 V; (d) Size: 20 nm x 20 nm, I = 25 pA, V = 1.0 V .

Methods

Scanning tunneling microscopy (STM) images have been obtained with a room-temperature STM (Scienta Omicron) attached to an UHV chamber with a base pressure of 1.0×10^{-10} mbar. All images were obtained in constant current mode and analyzed with the WSxM software.[S13] A Cu(111) surface was used as support for the molecules. Before deposition, the surface was cleaned by repeated cycles of Ar+ sputtering (1.0 kV) and annealing (450 ºC) until judged clean by STM. Nanographene molecule **1** was deposited from a 0.2 mM solution in CH_2Cl_2 using a pulsed-injection valve described elsewhere.[S12] To avoid contamination of the UHV chamber during deposition, the injection valve was installed in the fast entry lock (FEL), which has a base pressure of 5×10^{-8} mbar. Injection pulses in the range of milliseconds were applied in order to obtain submonolayer coverage. The pressure in the FEL increased to 10^{-2} mbar during the duration of the pulse, typically 5 ms.

References

(S1) I. R. Márquez, N. Fuentes, C. M. Cruz, V. Puente-Muñoz, L. Sotorrios, M. L. Marcos, D. Choquesillo-Lazarte, B. Biel, L. Crovetto, E. Gómez-Bengoa, M. T. González, R. Martin, J. M. Cuerva and A. G. Campaña, *Chem. Sci.*, 2017, **8**, 1068-1074.

(S2) D. Lungerich, J. F. Hitzenberger, M. Marcia, F. Hampel, T. Drewello and N. Jux, *Angew. Chem. Int. Ed.*, 2014, **53**, 12231-12235.

(S3) N. S. Makarov, M. Drobizhev and A. Rebane, *J. Opt. Soc. Am. B.*, 2008, **16**, 4029.

(S4) C. Xu and W. W. Webb, *J. Opt. Soc. Am. B.*, 1996, **13**, 481-491.

(S5) G. M. Sheldrick, *Acta Cryst.*, 2015, **A71**, 3-8.

(S6) G. M. Sheldrick, *Acta Cryst.*, 2008, **A64**, 112-122.

(S7) L. J. Farrugia, *J. Appl. Cryst.*, 2012, **45**, 849-854.

(S8) A. L. Spek, *Acta Cryst.*, 2015, **C71**, 9-18.

(S9) A. L. Spek, *Acta Cryst.*, 2009, **D65**, 148-155.

(S10) C.F. Macrae, P. R. Edgington, P. McCabe, E. Pidcock, G. P. Shields, R. Taylor, M. Towler, J. van de Streek and *J. Appl. Cryst.*, 2006, **39**, 453-457.

(S11) M. J. Frisch, G. W. Trucks, H. B. Schlegel, G. E. Scuseria, M. A. Robb, J. R. Cheeseman, G. Scalmani, V. Barone, B. Mennucci, G. A. Petersson, H. Nakatsuji, M. Caricato, X. Li, H. P. Hratchian, A. F. Izmaylov, J. Bloino, G. Zheng, J. L. Sonnenberg, M. Hada, M. Ehara, K. Toyota, R. Fukuda, J. Hasegawa, M. Ishida, T. Nakajima, Y. Honda, O. Kitao, H. Nakai, T. Vreven, J. A. Montgomery, Jr., J. E. Peralta, F. Ogliaro, M. Bearpark, J. J. Heyd, E. Brothers, K. N. Kudin, V. N. Staroverov, T. Keith, R. Kobayashi, J. Normand, K. Raghavachari, A. Rendell, J. C. Burant, S. S. Iyengar, J. Tomasi, M. Cossi, N. Rega, J. M. Millam, M. Klene, J. E. Knox, J. B. Cross, V. Bakken, C. Adamo, J. Jaramillo, R. Gomperts, R. E. Stratmann, O. Yazyev, A. J. Austin, R. Cammi, C. Pomelli, J. W. Ochterski, R. L. Martin, K. Morokuma, V. G. Zakrzewski, G. A. Voth, P. Salvador, J. J. Dannenberg, S. Dapprich, A. D. Daniels, O. Farkas, J. B. Foresman, J. V. Ortiz, J. Cioslowski and D. J. Fox, *Gaussian 09, Revision B.01 and C.01, Gaussian, Inc., Wallingford CT* 2010.

(S12) J. M. Sobrado and J. A. Martín-Gago, *J. Appl. Phys.*, 2016, **120**, 145307.

(S13) I. Horcas, R. Fernandez, J. M. Gomez-Rodriguez, J. Colchero, J. Gomez-Herrero and A. M. Baro, *Rev. Sci. Instrum.*, 2007, **78**, 013705.